Colloid Polym Sci (2016) 294:2051–2070
DOI 10.1007/s00396-016-3970-z

ORIGINAL CONTRIBUTION

A post-metallocene titanium(IV) complex bearing asymmetric tetradentate [ONNO]-type amino acid-based ligand and its activity toward polymerization of polar monomers at room temperature in aqueous emulsion

K. Sharma[1] · **Sudip K. De**[1]

Received: 27 April 2016 / Revised: 14 September 2016 / Accepted: 15 October 2016 / Published online: 28 October 2016

Abstract Due to increasing environmental concern regarding detrimental effects of organic solvents, a new post-metallocene titanium-based catalyst [$TiLCl_2$] {*LH_2=2-(3,5-Di-tert-butyl-2-hydroxy-benzylamino)-succinamic acid*} with sidearm approach has been synthesized for aqueous emulsion polymerization of olefins. The catalyst has been characterized by elemental analysis, ^{1}H NMR, ^{13}C NMR, HRMS, IR, and UV–visible spectroscopy. The catalyst is easy to synthesize and is moderately stable in water. In aqueous emulsion, in the presence of co-catalyst $NaBPh_4$, it has been found to exhibit moderate to high activity in the range of 10^4 to produce homopolymers and copolymers of methyl acrylate and methyl methacrylate which are widely used for a variety of applications. The influence of the main reaction parameters on the polymerization reactions at room temperature was studied including the catalyst/co-catalyst ratio, type of monomers, reaction time, etc. Structures and properties of the obtained polymers were analyzed by various instrumental techniques like differential scanning calorimetry (DSC), gel permeation chromatography (GPC), ^{1}H NMR, ^{13}C NMR, etc., as well as by various experimental methods. The results indicated that the PMMA and PMA produced by the newly synthesized catalytic system are syndiotactic rich and possess ultrahigh-viscosity average molecular weight in the order of 10^6 g/mol.

Keywords Early transition metal · Post-metallocene catalyst · Aqueous polymerization · Viscosity average molecular weight · Polymethyl methacrylate · Polymethyl acrylate

Introduction

With the vast economic importance of polyolefins, which is reflected by an annual production of more than 70 million tons of polyethylene and polypropylene, a versatile process called "emulsion polymerization" for nonpolar olefins came into the limelight [1]. The emulsion polymerization process involves the formation of stable latex with numerous applications, and the environmental friendliness and nonflammability of water are particularly advantageous. The free radical initiator method is one of the extensively followed operations for the production of stable aqueous dispersions [2] of surfactant-stabilized polymer microparticles in the range of 50 to 1000 nm diameter [3].

However, of all the conventional polymerization methods, transition metal-catalyzed coordination polymerization propounds the broadest scope of microstructure control. Properties such as stereoregularity, comonomer incorporation and tacticity, molecular weight, and molecular weight distributions can be controlled by the catalyst structure [4]. Earlier, most of these polymerization processes were catalyzed by transition metal complexes soluble in organic solvents [5]. Transition metal-catalyzed coordination polymerization in aqueous medium has received comparatively little attention. Carrying out such reactions in water is a highly attractive goal [6]. Bauers et al. [7] and Tomov et al. [8] have recently reported the successful polymerization of ethylene in water by neutral nickel(II) complexes.

Over the last two decades, this field has been dominated by metallocene complexes of group IV metals. Recently, much

Electronic supplementary material The online version of this article (doi:10.1007/s00396-016-3970-z) contains supplementary material, which is available to authorized users.

✉ Sudip K. De
sudipkde@gmail.com

[1] Department of Chemistry, Jaypee University of Engineering and Technology, Guna 473226, India

attention has been paid to the nonmetallocene catalysts, which include early [9], middle [10], and late transition metals [11] and lanthanide species incorporating nonmetallocene-based ligands. To develop a novel nonmetallocene catalyst, a crucial step is the control of the coordination pattern between metal and ligands to tune the electronic properties and steric hindrance of the active site [12]. Also, the oxophilic nature of early transition metals brings the idea of incorporating ligands containing relatively hard nitrogen and oxygen donors in the catalyst systems to make the catalytic complex more stable and active.

Monoanionic phenoxy-imines are the most versatile ligands to have emerged in olefin polymerization catalysis over the past 5 years or so [10]. Extensive work related to the ligand system has been reported in order to realize tailoring of polymer microstructure involving [N,N], [N,N,N], [N,O] [N,N,O], and [N,S,O] [13]. Kol et al. had introduced a series of tridentate [ONO] and tetradentate [ONNO] ligand systems which are suitable for the synthesis of isotactic polyolefins [14]. Tetradentate bis(phenolate) ligands of the type [OYYO] (Y = heteroatom donor N, P, S, or O) have attracted interest because they might mimic the steric environment of the surface Ti atoms in classical heterogeneous Ziegler Natta systems used for industrial production of isotactic polypropylene [15]. Furthermore, the steric and electronic properties of the [OYYO] ligands can be easily modulated.

Along with the type of ligand system for organic synthesis, a sidearm approach has also proven to be an efficient strategy for the design of organometallic catalysts. Gibson et al. reported that the activities of the catalysts, containing ligands with pendant donors, were higher than those of the corresponding catalysts without sidearm donors [10]. A study on asymmetric catalysis also found strong sidearm effects on selectivity and catalytic activity in some reactions [16]. The significance of the pendant arm has been emphasized because it is proposed to play a crucial role in determining the rates of the propagation and termination processes, thought to remain attached to the catalytic site, and is instrumental in achieving high activities [17].

On the basis of phenoxy-imine backbone and the role of the side arm, a series of titanium complexes with tridentate monoanionic [O¯NXR] (X = O, P, S, Se; R = alkyl, aryl) and dianionic [O¯NS¯] ligands with pendant donor groups have been reported in olefin polymerization. To date, all these high-performance nonmetallocene complexes are found to be efficient for polymerization of nonpolar vinyl monomers (α-olefins in particular) in organic solvent. Also, methylaluminoxane (MAO) is used as an activating agent for most of the reactions. However, it was demonstrated that $AlMe_3$ included in MAO can cause deactivation of phenoxy group-based nonmetallocene catalysts by an attack on a phenoxy-O group; moreover, MAO is found to be toxic [18]. Therefore, the emerging appeal is to develop early transition metal-based nonmetallocene catalysts for aqueous polymerization of polar monomers because, owing to their high oxophilicity, such catalysts have generally proven incompatible with functionalized vinyl monomers in achieving single-site controlled insertive aqueous polymerization of olefins [19, 20]. Poly(acrylates), poly(methacrylates), and acrylic formulation based on alkyl acrylate copolymers are of practical and commercial interest due to their number of unique features, for example, outstanding chemical and optical properties, stability of properties at severe conditions, resistance to weathering and moisture, high surface resistance, and many more [21].

Earlier, one titanium(IV) complex bearing a [ONO]-type tridentate ligand having an enantiomerically pure amino acid (L-valine) has been reported to be highly efficient for aqueous polymerization of polar and nonpolar olefins [22]. Recently, a new titanium(IV) complex, dichlorobis(salicylato) titanium(IV) [TiL_2Cl_2] (1){LH = salicylic acid} [23] bearing a tetradentate [OOOO]-type ligand, has been synthesized and characterized which is even cheaper and easier to synthesize and is also found to be more active for polymerization in the aqueous medium. Inspired by the success of this type of tetradentate ligand-based catalytic system and the reports on the beneficial effects of an additional donor groups like oxygen on the catalytic activity, we have designed a new tetradentate [ONNO]-type ligand introducing L-asparagine in place of L-valine and also replacing O-donor with N-donor in the side arm. The amino N is expected to provide an increased stabilization to the reactive, electron-deficient metal center. Herein, we report the synthesis, characterization, and study of the efficacy of water-soluble new amino acid (L-asparagine)-based titanium(IV) complex, $TiLCl_2$ {*LH_2=2-(3,5-Di-tert-butyl-2-hydroxy-benzylamino)-succinamic acid*} for polymerization of polar olefins (methyl acrylate and methyl methacrylate) at room temperature in aqueous emulsion. In addition, copolymerization of acrylates was also studied because of their good mechanical, optical, and thermal properties.

Materials and methods

General remarks

The ligand {*LH_2=2-(3,5-Di-tert-butyl-2-hydroxy-benzylamino)-succinamic acid*} was synthesized by modified Mannich reaction between L-asparagine, formaldehyde, and 2,4-Di-tert-butyl phenol. L-Asparagine was purchased from Molychem. Tetrahydrofuran, also purchased from Molychem, was dried by refluxing with sodium and benzophenone and freshly distilled prior to use. Titanium tetrachloride (anhydrous fuming liquid, extra pure), sodium n-dodecyl sulfate (SDS), and sodium tetraphenylborate were obtained from Loba Chemie and were used without purification.

Methyl acrylate and methyl methacrylate were purchased from Molychem and Loba Chemie, respectively, and were purified prior to use by the usual method.

No human and animals were involved in the present study.

Characterizations

^{1}H and ^{13}C NMR spectra were recorded on a Bruker 400-MHz spectrometer. Chemical shift values (δ) are reported in parts per million and calibrated to tetramethylsilane ($\delta = 0.00$). All NMR spectra were recorded at ambient temperature (298 K) unless otherwise noted. Elemental analyses were performed using Perkin Elmer Instruments 2400 Series II CHNS/O Analyzer. UV–visible spectra of the complex were recorded in methanol on a Shimadzu UV-1700 spectrophotometer. Fourier transform infrared (FT-IR) spectra were recorded using KBr pellets on a Thermo Nicolet FTIR Spectrometer (Nexus 870). Molecular weights and polydispersities of the polymers synthesized were determined using a Waters' gel permeation chromatography (GPC) system equipped with a M515 HPLC pump, three Styragel 4.6 × 300-mm columns connected in series [Waters' Styragel HR 5E (molecular weight range 10^3–10^7), Styragel HMW 7 (molecular weight range 10^5–10^8), and Styragel HMW 6E (molecular weight range 10^3–10^7)], and a M2414 RI detector. Commercially available HPLC-grade tetrahydrofuran (THF) served as the mobile phase and was delivered at a flow rate of 0.3 mL/min. Sample concentrations were 5 mg/mL in THF, and the injection volume was 20 μL. The detector signals were simultaneously recorded, and average molecular weights were calculated using Breeze software. Calibrations were done with narrow polymethylmethacrylate standards. HRMS has been obtained on a Micromass Q-Tof micro mass spectrometer. Differential scanning calorimetry (DSC) measurements were conducted on a DSC Q20 V24.11 Build 124. Accurately weighed samples (3–3.5 mg) were placed in hermetically sealed aluminum pan (40 μL) and scanned from 5 to 500 °C at a heating rate of 5 °C/min under a dry nitrogen atmosphere (flow rate 50 mL/min). The data were managed by TA Universal analysis.

Synthesis of ligand {LH_2=2-(3,5-Di-tert-butyl-2-hydroxy-benzylamino) -succinamic acid}

The dianionic tetradentate ligand {*LH_2=2-(3,5-Di-tert-butyl-2-hydroxy-benzylamino)-succinamic acid*} was synthesized following Mannich reaction (Scheme 1). The 2-amino-3-carbamoylpropanoic acid (L-asparagine, 3 g; 0.019 mol) was dissolved in aqueous solution of NaOH (50 mL containing 0.038 g; 0.019 mol). To this, 37 % aqueous formaldehyde (2.97 mL; 0.039 mol) was added and stirred for 20 min. In another round-bottom flask, 2,4-di-tert-butylphenol (4.12 g; 0.019 mol) was dissolved in 80 mL ethanol. The 2,4-di-tert-butylphenol solution was then added slowly to the basic solution of L-asparagine along with continuous stirring. After complete transfer of 2,4-di-tert-butylphenol solution, the reaction mixture was condensed for 24 h. The reaction mixture was then cooled to 4 °C and acidified by adding dilute HCl dropwise with continuous stirring, resulting in precipitation of a white semisolid product. The product was then filtered out, washed with distilled water and hexane, dried, and recrystallized from ethanol to give the ligand in 60 % yield. The ligand was characterized by ^{1}H NMR and ^{13}C NMR. ^{1}H NMR values (400 MHz, $CDCl_3$, ppm) are as follows: δ 1.26 ppm (s, 9H, *Ph-C(CH_3)$_3$*) and 1.40 ppm (s, 9H, *Ph-C(CH_3)$_3$*), 2.86 ppm (m, 2H, C*H_2*-$CONH_2$ J = 5.2 Hz), 3.80 ppm (s, 2H, *Ph-CH_2-NH*), 3.98 ppm (dd,1H, NH-C*H*COOH J = 4.8 Hz), 7.06 ppm (d, 1H, *Ph* J = 1.6 Hz), 7.28 ppm (d, 1H, *Ph* J = 1.6 Hz). ^{13}C NMR values are as follows: δ 25.63 and 34.29 (4° carbons Ph-*C* (CH_3)$_3$), 29.70, 31.66 (−C(*C*H_3)$_3$) of two t-but group, 34.77 (*C*H_2 ($CONH_2$), 44.89 (*C*H_2(NH), 62.11 (NH*C*H (COO), 123.50–152.06 (*Ph* Carbons), 177.01 (−CH*C*OO), 177.42 (H_2CCONH_2).

Synthesis of $TiLCl_2$ {LH_2=2-(3,5-Di-tert-butyl-2-hydroxy-benzylamino) -succinamic acid}

The ligand (3.96 g; 0.011 mol) and $TiCl_4$ (1.29 mL; 0.011 mol) were dissolved separately in 25 mL dry tetrahydrofuran under nitrogen atmosphere by continuous stirring in two different round-bottom flasks. The ligand solution was then added slowly and anaerobically to the solution of $TiCl_4$. The reaction mixture immediately turned dark red. Stirring was continued for one more hour, and then the solvent (THF) was removed under reduced pressure. The residue was recrystallized from toluene to obtain a dark red crystalline solid (**1**) (Scheme 2) yield: 4.3 g (80.2 %). Analysis calculated for $C_{19}H_{28}O_4N_2TiCl_2$ (molecular weight = 467.21) is as follows: C, 48.8; H, 6.04; N, 6.00; found: C, 48.9; H, 6.05; N, 6.05. ^{1}H NMR (400 MHz, $CDCl_3$, ppm) values are as follows: δ 7.29 (d, 1H, *Ph* J = 1.2 Hz), 7.06 (d, 1H, *Ph*, J = 1.2 Hz), 4.05 (dd, 1H, NH*CH*COOH. J ~ 4.8 Hz), 3.84 (s, 2H, Ph-C*H_2*-NH), 2.88 (m, 2H, C*H_2*$CONH_2$, J ~ 4.2 Hz), 1.41 (s, 9H, Ph-C(C*H_3*)$_3$), 1.29 (s, 9H, Ph-C(C*H_3*)$_3$) (Fig. S1, Supporting Information). ^{13}C NMR values are as follows: δ 25.65 and 34.35 (4° carbons Ph-*C* (CH_3)$_3$), 29.79, 31.75 (−C (*C*H_3)$_3$) of two t-but group, 34.85 (*C*H_2 ($CONH_2$), 45.01 (*C*H_2(NH), 62.19 (NH*C*H (COO), 123.57–152.14 (*Ph* carbons), 177.12 (−CH*C*OO), 177.77 (H_2CCONH_2). Peaks in the range of 76.82–77.33 ppm appear due to the NMR solvent ($CDCl_3$) (Fig. S2, Supporting Information).

Scheme 1 Synthesis of ligand, 2-(3,5-Di-tert-butyl-2-hydroxy-benzylamino)-succinamic acid}

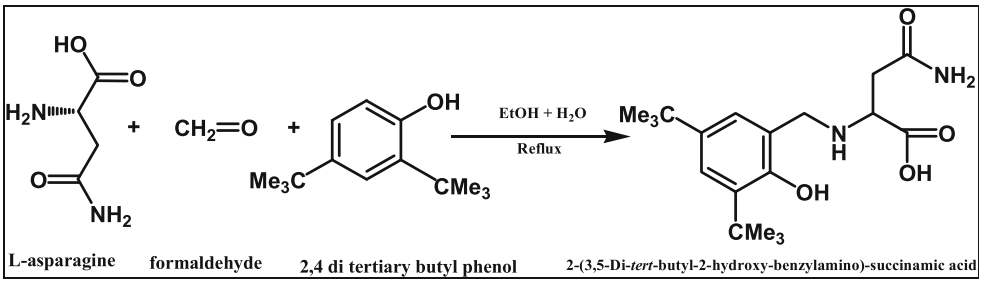

Polymerization reactions

All polymerization reactions were carried out at room temperature (25 °C) in the presence of air. Commercially obtained polar monomers, methyl methacrylate, and methyl acrylate were distilled prior to use.

Homopolymerization of MMA and MA

Aqueous homopolymerization reactions were carried out at room temperature (25 °C) in the presence of air. Sodium n-dodecyl sulfate (SDS) (0.233 g; 0.8 mmol) was dissolved in water (35 mL) and stirred for 15 min. To this, freshly distilled methyl methacrylate (1.81 mL; 0.02 mol) or methyl acrylate (2.2 mL; 0.02 mol) was added and stirred for one more hour. Simultaneously, in another round-bottom flask, complex 1 (0.05 g; 0.1 mmol) was suspended in water (15 mL) and stirred for 1 h to obtain a clear yellow solution. To the emulsified monomer solution, the aqueous solution of 1 was then added, followed immediately by $NaBPh_4$ (0.034 g; 0.1 mmol). The reaction mixture was then stirred at room temperature for the required time period to study the reaction kinetics. The reaction mixture was then quenched by pouring it into methanol to precipitate the polymer product. The product was than washed three to four times with water and dried in vacuum at ambient temperature.

Copolymerization of MMA and MA

Methyl methacrylate and methyl acrylate were copolymerized in a series of reactions with systematic variations in a molar ratio of methyl methacrylate (MMA) and methyl acrylate (MA), keeping a total amount of monomer fixed at 0.02 mol. Both the monomers were premixed and added simultaneously. The reaction mixture was stirred for 60 min, and then the reaction was terminated by pouring it into methanol. The precipitated copolymer was then filtered, washed repeatedly with water, and dried in a vacuum at ambient temperature. The copolymer was further purified by dissolving it in chloroform and then reprecipitating it by the addition of methanol and finally dried in a vacuum. Monomer reactivity ratios are important quantitative values to predict the copolymer composition and mechanistic aspects of copolymerization. Monomer reactivity ratios are generally determined at low conversion. Therefore, a set of five experiments were conducted wherein different feed ratios of methyl methacrylate and methyl acrylate were employed and copolymerization reactions were quenched at low yields (<10 %). The copolymer composition was calculated using ^{1}H NMR, and the reactivity ratio was calculated by Fineman–Ross and Kelen–Tudos least square methods.

Results and Discussion

In general, catalysts containing oxophilic/halophilic/Lewis acidic metals have proven incompatible with functionalized vinyl monomers in achieving polymerization of olefins bearing polar functional groups ("polar olefins") [19]. The goal of this research was to investigate the efficacy of the single-site homogeneous titanium-based catalytic system with a pendant group in the polymerization of polar olefins.

Scheme 2 Synthesis of the catalyst precursor $[TiLCl_2]$ (**1**)

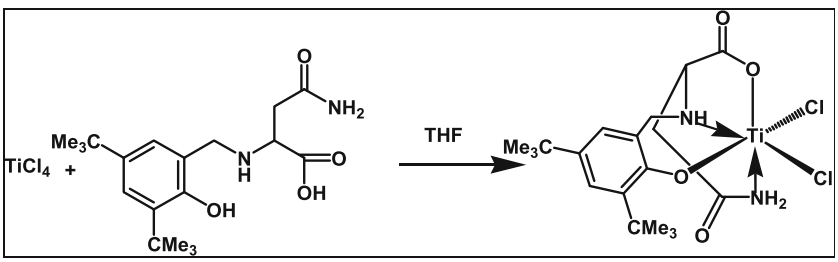

Synthesis and characterization of the ligand {LH_2=2-(3,5-Di-tert-butyl-2-hydroxy-benzylamino) -succinamic acid}

The ligand {*LH_2=2-(3,5-Di-tert-butyl-2-hydroxy-benzylamino)-succinamic acid*} was synthesized following Mannich-type condensation reaction in moderate yield (60 %). It was characterized by using ^{1}H NMR and ^{13}C NMR spectroscopy. The ^{1}H NMR spectrum (Fig. 1) of the ligand shows two peaks at 1.26 ppm (9H, s) and 1.40 ppm (9H, s) due to –CH_3 protons of the two t-butyl groups. The signal for the –CH_2 proton of the –C*H_2* ($CONH_2$) group appears at 2.86 ppm (2H, m; J = 5.2 Hz) and that of the –CH_2 proton of –C*H_2*NH group appears at 3.80 ppm (2H, s). The signal for the CH proton of the (NHC*H*(COOH) group appears at 3.98 ppm (1H, dd; J = 4.8 Hz). The broad peak at 5.15 ppm may be assigned to the phenolic –OH proton, and the peaks at 6.50 and 6.57 ppm appear for the nonequivalent protons of the CON*H_2* group. The signals for the aromatic protons appear at 7.28 ppm (1H, d; J = 1.6 Hz) and at 7.06 ppm (1H, d; J = 1.6 Hz). The small peak at 1.88 ppm may be due to the –NH proton of the –CH_2N*H* group.

The ^{13}C NMR spectrum [400 MHz, $CDCl_3$] (Fig. 2) of the ligand shows peaks at 25.63 and 34.29 ppm for the 4° carbons of the tertiary butyl groups. Peaks at 29.70 and 31.66 ppm appear for the methyl carbons –C(***C***H_3)$_3$ present in two t-butyl groups. Two sharp singlets at 34.77 and 44.89 ppm appear for (*C*H_2 ($CONH_2$) and CH_2 carbon of the *C*H_2 (NH) group. The peak at 62.11 ppm is for –CH carbon of the NH*C*H(COOH) group. Peaks at 123, 124, 125, 135, 142, and 152 ppm are for carbons of the phenyl ring. Peaks at 177.01 and at 177.42 may be assigned to carbonyl carbon of the (NHCH*C*OOH) and (H_2C*C*ONH_2) groups which appear downfield due to the deshielding effect of oxygen.

Synthesis and characterization of the complex 1[$TiLCl_2$] {LH_2=2-(3,5-Di-tert-butyl-2-hydroxy-benzylamino) -succinamic acid}

The ligand on reaction with $TiCl_4$ in dry THF afforded complex 1, [$LTiCl_2$], in good yield (80.2 %). Commercially available $TiCl_4$ reacts violently with water to produce a lot of heat and insoluble TiO_2. Therefore, synthesis of titanium complexes involving $TiCl_4$ is performed in dry organic solvents. Complex 1 was characterized by using different instrumental techniques like elemental analysis, ^{1}H NMR, ^{13}C NMR, HRMS, IR, and UV–visible spectroscopy. The proposed possible structure of the complex with formula $C_{19}H_{28}O_4N_2TiCl_2$ was well supported by elemental analysis (Table 1).

The ^{1}H NMR and ^{13}C NMR spectra (Fig. S1 and S2, Supporting Information) of the catalytic complex show all the characteristic peaks of the ligand. A slight downfield shift of the signals in the NMR spectra of the complex for protons and carbons from those of the ligand clearly supports that, in

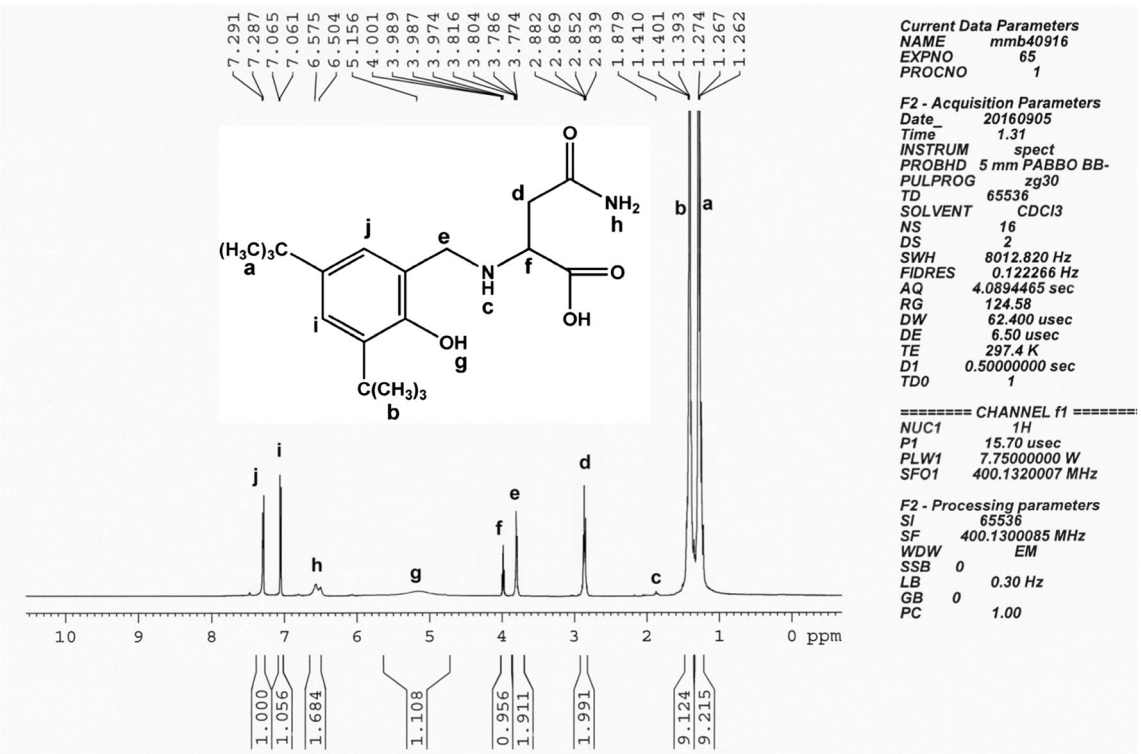

Fig. 1 ^{1}H NMR spectrum of **a** the ligand LH_2 in $CDCl_3$

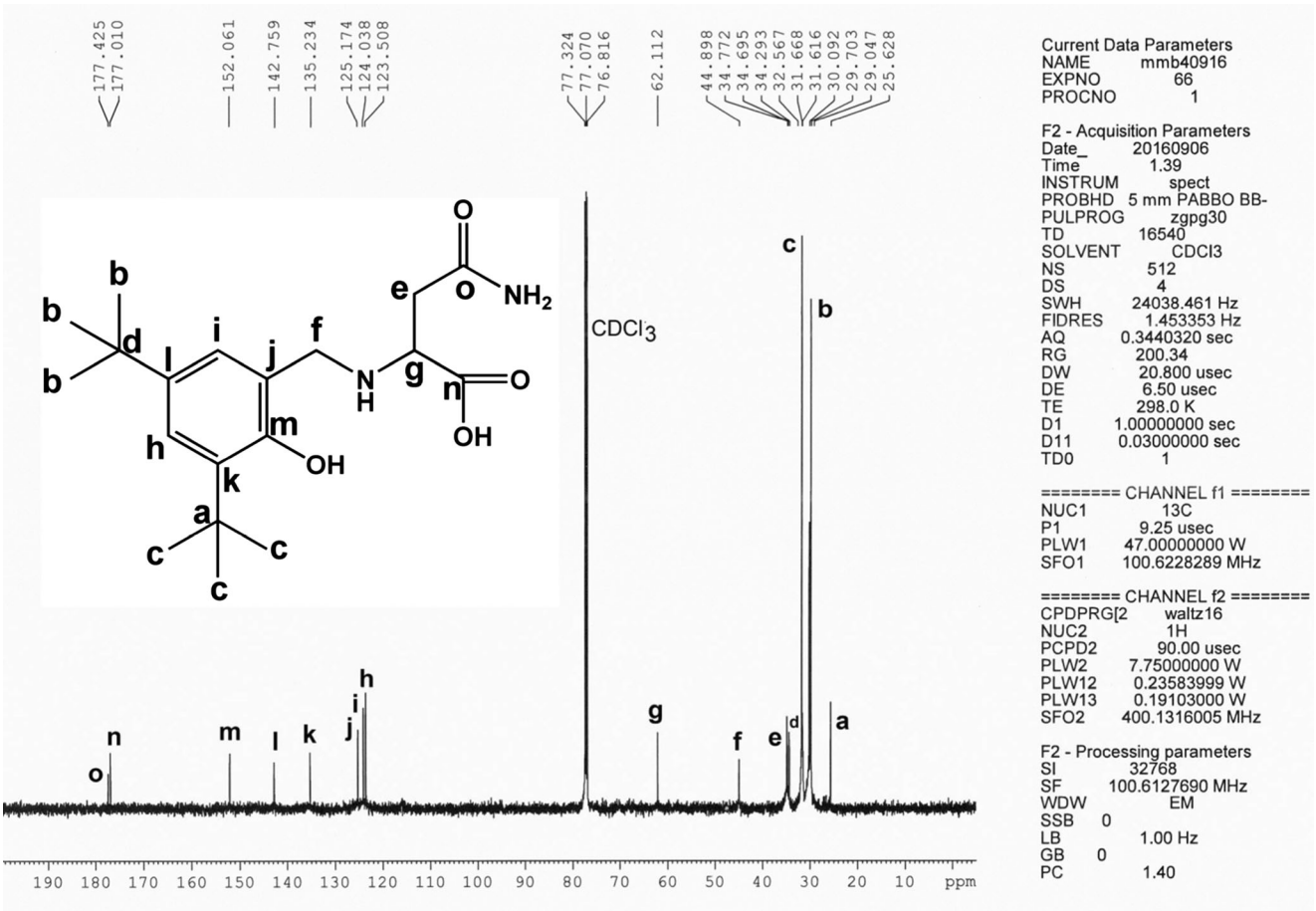

Fig. 2 ^{13}C NMR spectrum of **a** the ligand LH_2 in $CDCl_3$

the titanium complex, the ligand is coordinated to the titanium center. Consequently, ^{1}H NMR and ^{13}C NMR show good consistency with the assigned structure.

IR spectrum

The IR spectrum of complex 1 (Fig. 3) shows a band at 485.65 cm^{-1} which can be assigned to Ti–Cl stretching vibrations [24]. Involvement of the N in coordination to the metal center (*Ti*) is supported by the IR band at 585.48 cm^{-1}. Titanium bonded to carboxylate oxygen of the ligand shows band at 1410.38 cm^{-1}. The C–N and C–O stretching bands can be assigned to 1086.78 and 1237.30 cm^{-1}, respectively. The spectra of the complex show C–H stretching frequency at 2868 cm^{-1} for the tertiary butyl group. N–H stretching frequency appears in the range 3400–3300 cm^{-1}. Therefore, a broad band centered around 3346 cm^{-1} may be assigned to $\upsilon_{N\text{-}H(stretching)}$.

Table 1 Analytical data of the complex

	Formula	% C	% H	%N
Found	$C_{19}H_{28}O_4N_2TiCl_2$ [$LTiCl_2$]	48.90	6.05	6.05
Calculated		48.84	6.04	6.00

UV–visible spectrum

The UV–visible spectrum of the titanium complex 1 (Fig. 4) with 10^{-3} M concentration was recorded in methanol. The complex exhibits electronic transition at λ 350 nm (ε ~250) due to phenoxyl (acting as Lewis base) to titanium (acting as Lewis acid) charge transfer. The intense peak at λ 220 nm with ε value in the order of (2.26×10^3) can be assigned to intra-ligand $\pi \rightarrow \pi^*$ transition. Also, the spectrum of the complex shows a shift toward the higher-wavelength region in comparison to absorption bands for the free ligand system which is indirect evidence for the involvement of O and N atoms in coordination to the metal center [25].

The high-resolution mass spectrum (HRMS) (Fig. 5) of the complex shows a peak at *m*/*z* 489.0937 due to $C_{19}H_{28}Cl_2N_2O_4TiNa^+$. The isotope pattern also matches with the composition. The peak at *m*/*z* 373.2236 may be assigned to the ligand $C_{19}H_{30}N_2O_4Na^+$.

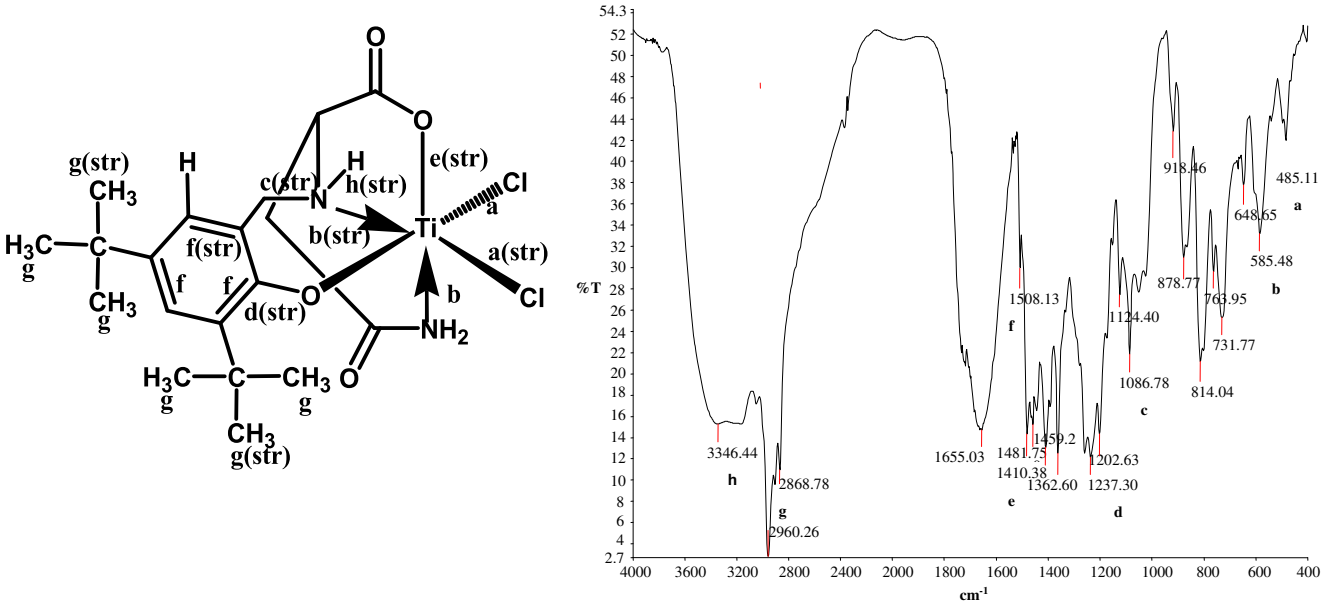

Fig. 3 IR spectrum of complex 1

Homopolymerization of MMA and MA

Most of the hard Lewis basic ligands having a charged oxygen donor stabilize Ti toward hydrolysis [26]. Studies on the stability and hydrolysis chemistry of metallocene dichloride complexes by Marks et al. in 1985 also reveal that addition of any Cp_2MCl_2 {M (IV) = hard acids like vanadium, titanium, and zirconium} complexes in water results in rapid chloride ion dissociation to give $[Cp_2M(OH)(OH_2)]^+$ as the major product and the approximate half-lives for loss of cyclopentadienyl anion being 57 h for Ti and 240 h for V complexes [27]. A nonmetallocene titanium(IV) complex bearing an asymmetric tridentate [ONO]-type ligand has also been reported to produce similar active species which exhibit similar catalytic behavior in the presence of a large, soft, and weakly coordinating anion BPh_4^- [28–30]. Therefore, we expected that the newly synthesized complex $[L_2TiCl_2]$ {*LH_2=2-(3,5-Di-tert-butyl-2-hydroxy-benzylamino)-succinamic acid*} upon addition to water will produce a similar $[L_2Ti(OH)(OH_2)]^+$ type of species which in the presence of $NaBPh_4$ should be capable of acting as polymerization catalyst. Our expectations proved to be correct as the present system was also found to produce poly(methy1 methacrylate) (PMMA) in good yield (87.0 %). To optimize the reaction parameters for polymerization of MMA, we carried out a number of control experiments using different concentrations of $NaBPh_4$ and complex 1 and the results are summarized in Table 2. The effect of the concentration of counteranion BPh_4^- has been studied first, and it has been found that, for higher yield, a Ti/B ratio of 1:1 is required (entry 1, Table 2) below which the conversion was found to be average (entry 2, Table 2), and when the Ti/B ratio of 1:2 was used, little change could be observed in yield (entry 3, Table 2). The effect of the concentration of the precatalyst was also studied, and it was concluded that, when 0.25 mol% catalyst loading (with respect to monomer) is used, the yield has been found to be average (entry 4, Table 2). Further increase in the concentration of the precatalyst from 0.25 to 0.5 mol% results in a surprisingly higher yield in the range of 80 % (entry 1, Table 2). Also, when 1 mol% Ti was used, not much increase in yield was noticed (entry 5, Table 2). In view of the higher yield of the polymer obtained, we decided to employ 0.5 mol% (with respect to monomer) of complex 1 and $NaBPh_4$ in the polymerization reactions. The individual role of the catalyst for polymerization reactions in the absence of counteranion $NaBPh_4$ and vice versa was also studied but failed to afford any polymer (entries 6 and 7, Table 2). Optimization of reaction parameters for polymerization of

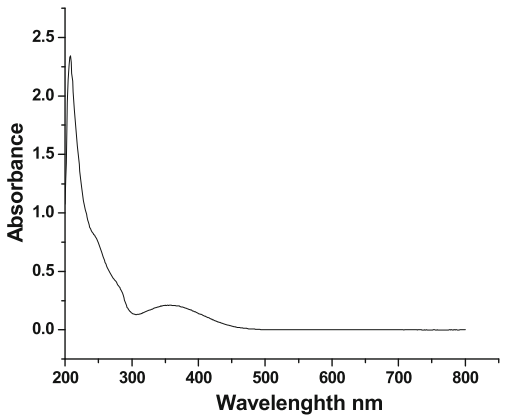

Fig. 4 UV–visible spectrum of complex 1 in methanol (10^{-3} M)

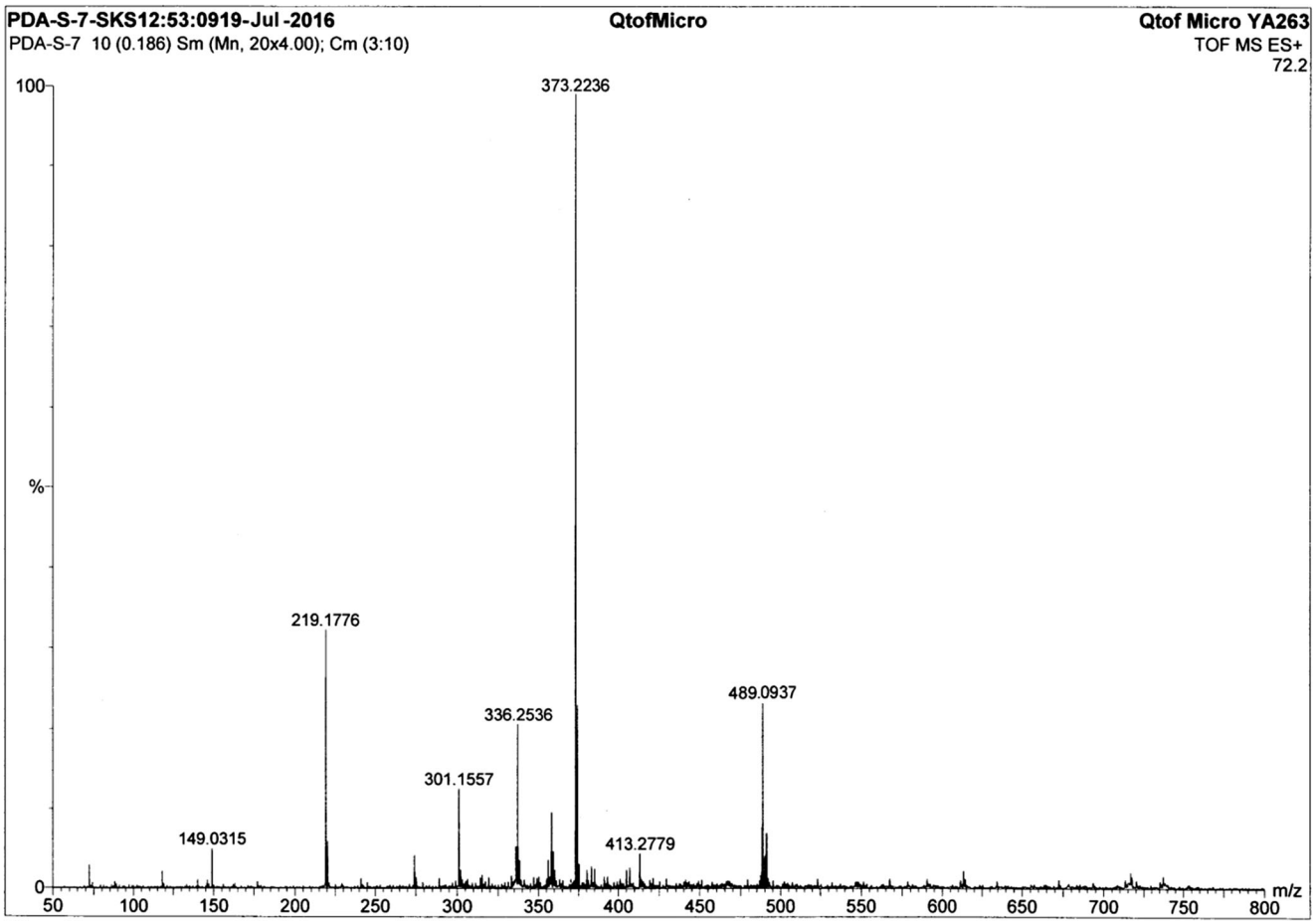

Fig. 5 High-resolution ESI-mass spectrum of complex 1

MA was carried out in a similar manner as for MMA, and the results are summarized in Table 2.

Similar trends were obtained in the case of polymerization of methyl acrylate, where the yield obtained was slightly higher with respect to the yield obtained in polymerization of MMA under identical reaction conditions.

With the optimized reaction parameters, the effect of polymerization times on the activity of the catalytic complex synthesized and on MMA and MA polymerization in the presence of air were studied. The results are summarized in Tables 3 and 4 and illustrated in (Fig. S3 to S6, Supporting Information).

Fujita and Coates introduced an important family of group 4 nonmetallocene catalysts based on the phenoxy-imine ligand system [31]. These catalysts bearing pendant donors are found to be highly efficient for polymerization reactions

Table 2 Optimization of homopolymerization of MMA and MA catalyzed by 1 in the presence of $NaBPh_4$ and air at room temperature (25 °C) in aqueous emulsion[a]

Entry	1 (mmol/L)	$NaBPh_4$ (mmol/L)	MMA, yield g (%)	MMA, yield g (%)
1	2	2	1.74 (87.0)	1.54 (88.3)
2	2	1	1.21 (60.5)	1.31 (76.1)
3	2	4	1.77 (88.39)	1.55 (90.0)
4	1	1	0.96 (48.0)	1.23 (71.4)
5	4	4	1.83 (91.5)	1.59 (92.3)
6	2	0.0	–	–
7	0.0	2	–	–

Reaction conditions: reaction time = 1 h, MMA and MA concentration = 0.4 mol/L (0.02 mol in 50 mL SDS/water)

Table 3 Homopolymerization of MMA catalyzed by 1 in the presence of $NaBPh_4$ and air at room temperature (25 °C) in aqueous emulsion[a]

Entry	Time (min)	M_n ($\times 10^5$)[a]	M_v[b] $\times 10^5$	M_w/M_n[a]	Yield g (%)	Activity ($\times 10^4$)[c]
1	5	5.10	7.9	1.6	0.98(49.0)	11.76
2	10	6.62	9.6	1.6	1.08(54.0)	6.48
3	20	6.54	10.5	1.6	1.30(65.0)	3.90
4	30	6.72	10.9	1.6	1.51(75.5)	3.00
5	60	7.22	11.4	1.7	1.74(87.0)	1.74
6	90	8.18	12.0	1.8	1.79(89.5)	1.19

Reaction conditions: [1] = [$NaBPh_4$] = 0.002 mol/L, MMA concentration = 0.4 mol/L (0.02 mol/50 mL SDS/water)

[a] GPC

[b] Viscosity average molecular weight

[c] Gram of polymer per mole of catalyst per hour

in contrast to the phenoxy-amine class of complex which shows low activity and high isotacticity for olefin polymerization [32]. Inspired by these reports, activity of the newly synthesized tetradentate phenoxy amine-based complex $[L_2TiCl_2]$ *{LH_2=2-(3, 5-Di-tert-butyl-2-hydroxy-benzylamino)-succinamic acid}* with hard donor (nitrogen) has been studied. It appears that as reaction time increases, the yield of the polymer product increases. But after some time, the yield of the product becomes almost constant (entries 5 and 6, Table 3) and (entries 4 and 5, Table 4). From the yield versus time plot (Fig. S3 Supporting Information), it appears that the polymerization reactions are faster for MA producing 87.1 % polymer product within 30 min whereas in the case of MMA, the yield increases to 87.0 % after 60 min. Further increase in polymerization time results in no major difference in yield (entry 6 Table 3) and (entry 5 Table 4). Unlike the increase in yield with time, the longer polymerization time shows a detrimental effect on catalyst activity (Fig. S4 Supporting Information) This is because the catalyst slowly undergoes decomposition by hydrolysis with time which was further confirmed by the fact that the orange yellow color of the polymerization mixture started to fade slowly with time. In comparison to the activity (10^3) of the earlier reported phenoxy-amine ligand-based titanium complex in the presence of argon [21], this new complex bearing extra nitrogen as a pendant donor is found to be highly active even in the presence of air with activity in the range of 10^4.

Homopolymers of functionalized monomers, methyl acrylate, and methyl methacrylate have been characterized by ^1H NMR, ^{13}C NMR spectroscopy, GPC, and DSC and by experimental techniques. Interesting, unique and most of the advantageous properties of polymer materials depend upon its average molecular weight. GPC and experimental methods were used to find out the average molecular weight of the polymers. Viscometry is a useful experimental technique for calculating the viscosity average molecular weight, M_v. In the early 1930s, Staudinger used viscosity as a measure of the molecular weight of the polymer. He proposed the relationship ($\eta_{sp} = K_s Cm$) to postulate his hypothesis about the long-chain polymer molecules. Later, to obtain the molecular weight from limiting the viscosity number, Staudinger equation was replaced by the famous and well-known Mark–Houwink equation [33].

$$[\eta] = \mathrm{K}.(M_v)^{\mathrm{a}} \left(\text{acetone at } \overset{\circ}{\underset{}{30}}\mathrm{C} \right) \quad (1)$$

where value of a and K are constants for a given polymer/solvent/temperature system. Viscosity average molecular

Table 4 Homopolymerization of MA catalyzed by 1 in the presence of $NaBPh_4$ and air at room temperature (25 °C) in aqueous emulsion [a]

Entry	Time (min)	M_n ($\times 10^6$)[a]	M_v[b] $\times 10^6$	M_w/M_n[a]	Yield g (%)	Activity ($\times 10^4$)[c]
1	5	1.14	5.6	1.6	1.02(59.2)	12.24
2	10	1.68	5.9	1.4	1.11 (64.4)	6.66
3	20	2.23	8.1	1.6	1.27 (73.7)	3.81
4	30	5.38	8.3	1.6	1.50 (87.1)	3.02
5	60	6.33	9.5	1.7	1.54(89.4)	1.54
6	90	6.53	9.8	1.7	1.60(92.9)	1.06

Reaction conditions: [1] = [$NaBPh_4$] = 0.002 mol/L, MA concentration = 0.4 mol/L (0.02 mol/50 mL SDS/water)

[a] GPC

[b] Viscosity average molecular weight

[c] Gram of polymer per mole of catalyst per hour

weights of homopolymers PMA and PMMA were calculated by finding specific and reduced viscosities experimentally in acetone solution at 30 °C using an Ostwald viscometer with a flow time of 0.83 min for pure acetone. From the concentration versus viscosity plot, the value for limiting viscosity was found and put in the Mark–Houwink equation to calculate M_v of different polymeric samples. Viscosity average molecular weights (M_v) of the polymer samples, determined experimentally, have been found to be in the range of 7.9×10^5 to as high as 9.8×10^6 (Fig. 6) From the yield versus M_v plot (Fig. S5, Supporting Information), it is concluded that with increase in yield, M_v also increases. The same trend is observed from the time versus M_v plot (Fig. S6, Supporting Information). It is noted that as the polymerization time increases, viscosity average molecular weight (M_v) also increases. The number average molecular weights obtained from GPC range from 5.1×10^5 to as high as 6.53×10^6 with PDI values ranging from 1.4 to 1.8 (Fig. 7).

NMR spectroscopy is one of the most convenient instrumental techniques for resolving chemical structures of the polymers. The ^{1}H NMR spectrum (Fig. 8) shows resonances at 3.52 and 2.03 ppm for methoxy and methylene protons. The triad tacticities were determined by using the area ratios of α-methyl proton-splitting peaks in ^{1}H NMR spectra. Methyl triad distribution of PMMA shows that PMMA samples are syndiotactic rich, the average composition being [rr] = ca. 64 %, [mr] = ca. 32 %, and [mm] = ca. 4 %. The stereochemistry of the polymerization is chain-end controlled as evidenced by the triad tests $\{4[rr][mm]/[mr]^2 \approx 0.87\}$.

The ^{13}C NMR spectrum (Fig. S7, Supporting information) of PMMA shows peaks at 16.55 and 18.73 ppm due to α-CH_3 carbons of [rr] and [mr] triad sequences. The quaternary carbons of [rr] and [mr] triads appear at 44.56 and 44.90 ppm, respectively. The relative intensities of these peaks also suggest that the PMMA samples are syndiotactic rich. The peak for –OCH_3 carbon appears at 51.79 ppm and that for CH_2 carbon appears at 54.17–54.39 ppm. The signal for –C=O carbon appears at 176.98–178.09 ppm. The peaks at 176.98, 177.79, and 178.09 ppm can be assigned to [mmrr + rrmr], [rrrr], and [rrrm] pentad sequences [34]. The exact structure of the PMMA sample was supported by ^{13}C NMR which shows

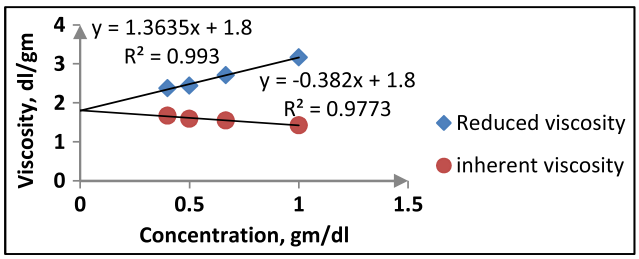

Fig. 6 Concentration versus limiting viscosity numbers (η) plot of PMMA

that the PMMA sample synthesized by complex 1 was free from impurities [35].

The ^{1}H NMR spectra of PMA samples (Fig. 9) show peaks in the region 1.41–1.94 ppm for –CH_2 protons. The cross peaks around 1.93 and 1.47 ppm are assigned to the meso (*m*) dyad, and the cross peaks around 1.68 ppm are assigned to the racemic (*r*) dyad of the methylene proton. Matsuzaki et al. [36] have reported that in NMR spectra of PMA, the resonance signals due to methylene protons in syndiotactic configurations overlap with signal due to one of two methylene protons in the isotactic configuration region. A similar overlap in signals is found in the NMR spectrum of PMA which is evidence in support of the syndiotactic-rich polymeric product. A small peak with low intensity at 2.31 ppm can be assigned to –CH proton [37]. A sharp singlet for methoxy proton (−OCH_3) appears at 3.66 ppm. Peak at 7.26 ppm can be assigned to $CDCl_3$. The ^{13}C NMR spectrum of polymethyl acrylate is also studied, and details are given in Fig. S8, Supporting Information.

Glass transition temperature

Syndiotactic-rich polymeric materials are reported to exhibit higher glass transition temperature (T_g) and hence are good for higher-temperature applications [38]. The syndiotactic-rich microstructure of PMA and PMMA was also supported by thermal analysis (DSC). The glass transition temperature of homopolymers was measured by differential scanning calorimetry, under the N_2 atmosphere. This technique controls heat flow associated with phase transitions as a function of temperature. The glass transition temperature of a phase transformation is very important in the case of polymers because all the mechanical properties of the polymers are influenced by glass transition temperature. Polymethyl acrylate is a hydrophobic synthetic polymer with low T_g of ~9 °C [39] as reported in the literature. DSC analysis reveals higher T_g of ~23 °C for PMA (Fig. 10), which supports the higher syndiotactic content and higher molecular weight of the polymeric product. A similar result was reported for homopolymers of PMMA; high syndiotacticity imparts higher glass transition temperature of ~136 °C (Fig. 11).

Copolymerization of MMA and MA

Monomers like MMA, MA, n-tertiary-butyl acrylates, vinyl halides, etc., and their polymers are associated with distinctive properties. Functional groups provide subsequent refinement of polymers for specific applications [40]. Optical clarity is the chief characteristic of acrylate-type polymers. Acrylate polymers and copolymers are frequently used in the construction of adhesives and pressure-sensitive adhesives. Due to high transmittance, good mechanical properties, and thermal resistance, acrylic copolymers are used in the manufacture of

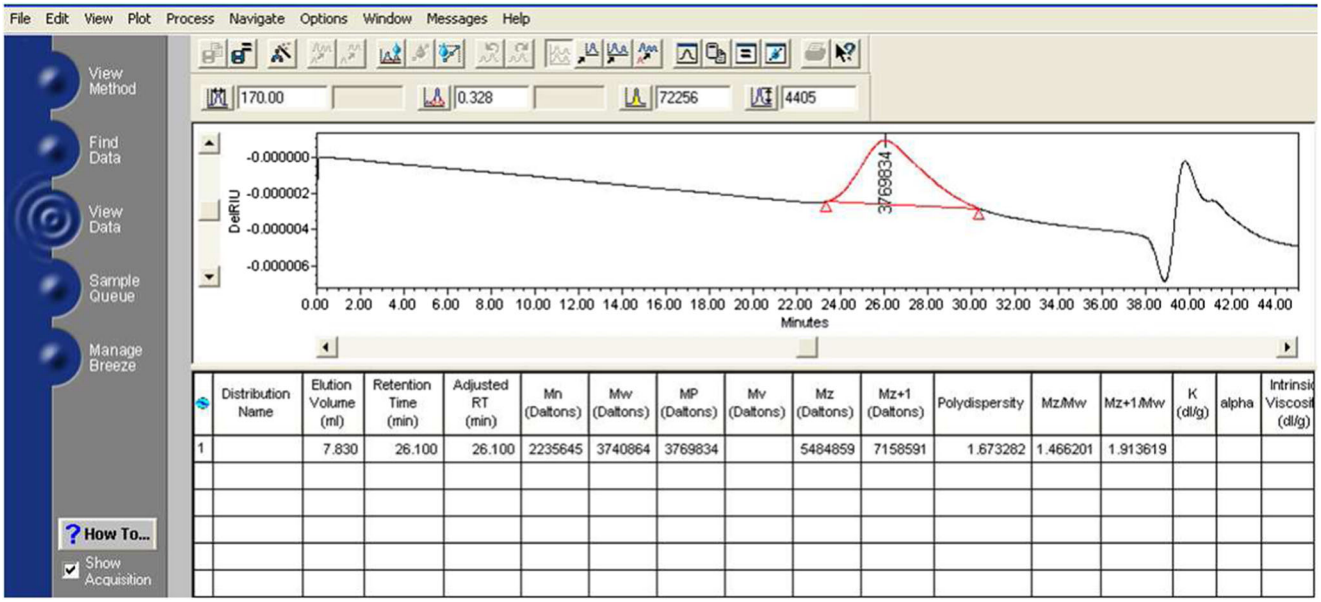

	Distribution Name	Elution Volume (ml)	Retention Time (min)	Adjusted RT (min)	Mn (Daltons)	Mw (Daltons)	MP (Daltons)	Mv (Daltons)	Mz (Daltons)	Mz+1 (Daltons)	Polydispersity	Mz/Mw	Mz+1/Mw	K (dl/g)	alpha	Intrinsic Viscosity (dl/g)
1		7.830	26.100	26.100	2235645	3740864	3769834		5484859	7158591	1.673282	1.466201	1.913619			

Fig. 7 Representative GPC of PMMA

plastics, woven and non-woven textiles, film coatings, and leather finishes, particularly nubuck and suede [41]. In the year 1998, due to interesting morphological, phase, and mechanical properties of such polymers, the challenging task of synthesizing block copolymers of acrylates and methyl acrylates came into the limelight. Of the several conventional polymerization techniques, the atom transfer radical polymerization (ATRP) technique was used [42].

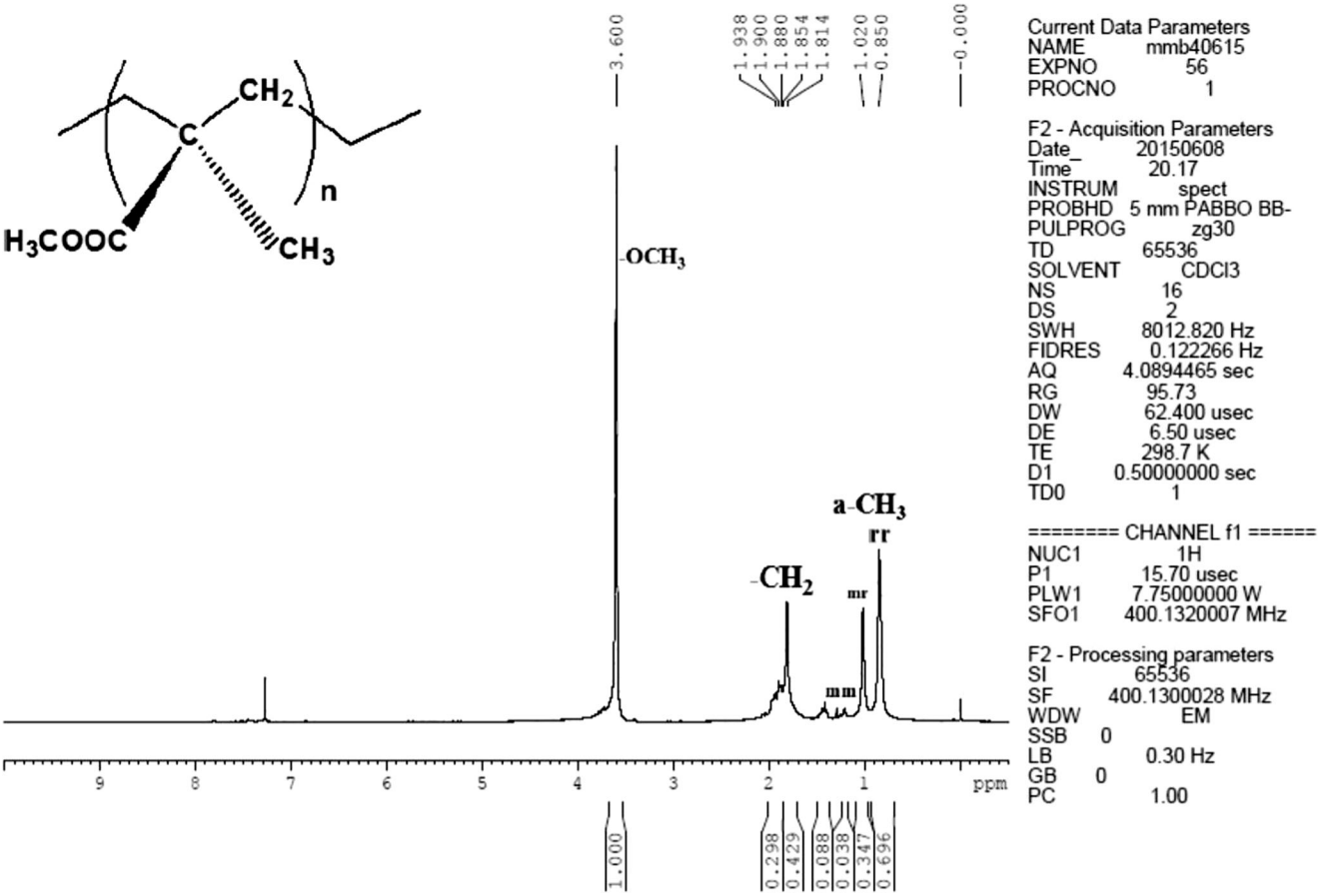

Fig. 8 Representative ^{1}H NMR spectrum of PMMA synthesized

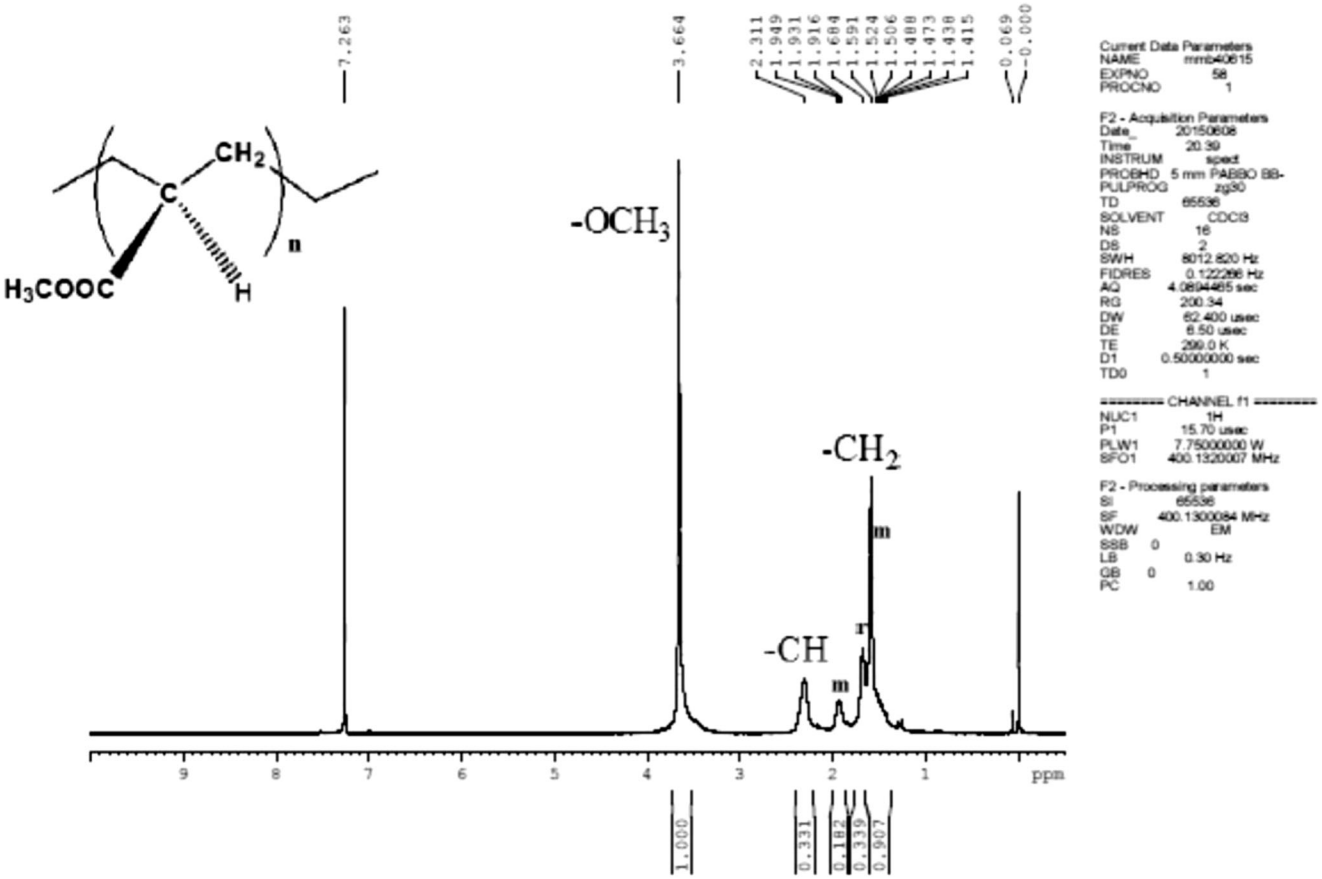

Fig. 9 Representative ^{1}H NMR spectra of PMA synthesized

Conversely, early transition metal catalysts were regarded as unpromising for such copolymerization. This is because early transition metal catalysts are highly oxophilic in nature and thus deactivated by the presence of polar monomers in polymerization medium [43]. Therefore, as a challenge, we have carried out a number of copolymerization reactions of

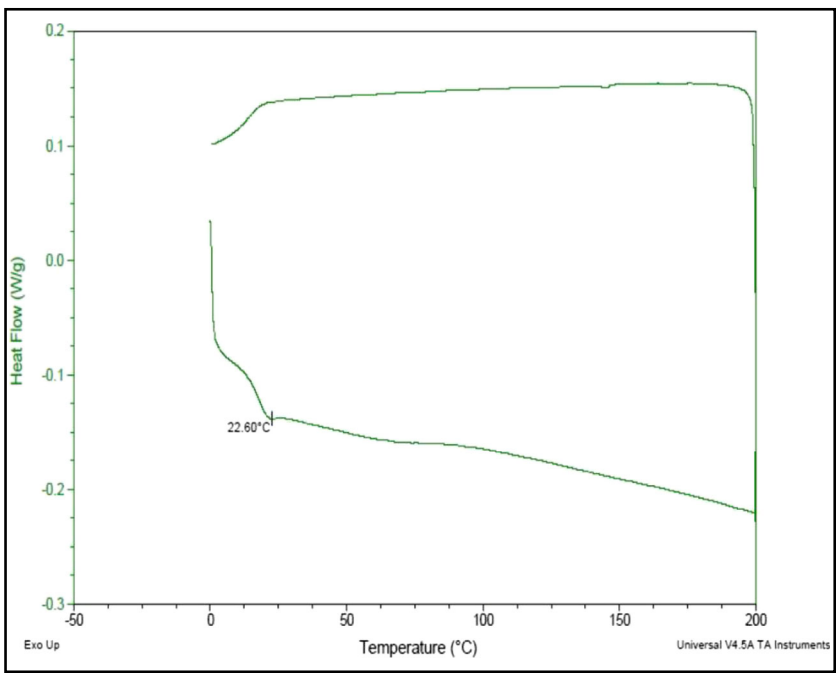

Fig. 10 DSC curve of polymethyl acrylate

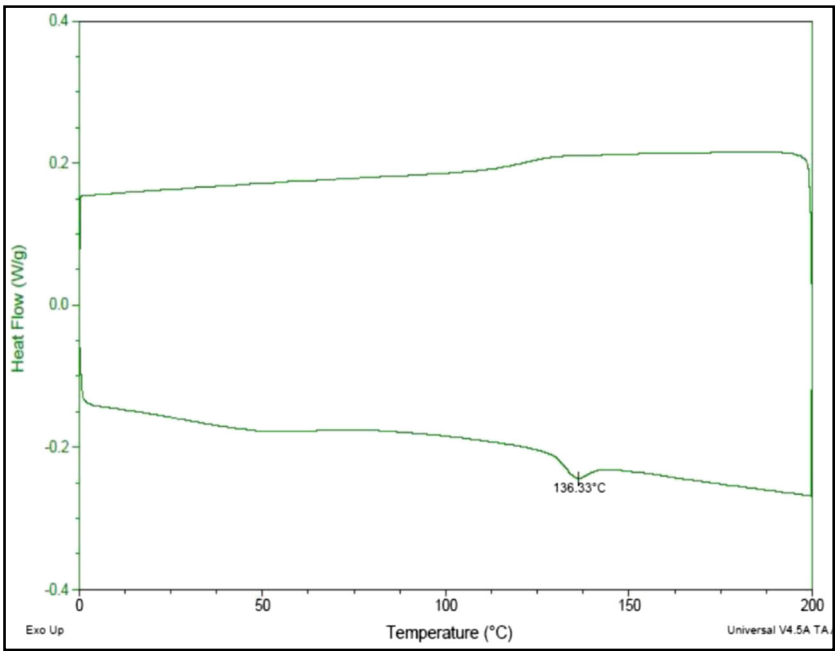

Fig. 11 DSC curve of polymethyl methacrylate

the polar monomers (MMA and MA) by complex 1 to check the activity and efficiency of the synthesized post-metallocene catalytic system.

Copolymerization reactions were carried out using varying feed ratios of MA and MMA at room temperature using $LTiCl_2$ as a catalyst and $NaBPh_4$ as a co-catalyst in the presence of SDS. Both the monomers were premixed and added simultaneously. The percentage of methyl methacrylate incorporation was determined by using the formula $(A_{\alpha\text{-}methyl} / A_{O\text{-}CH3}) \times 100$ where $A_{\alpha\text{-}methyl}$ is the area of MMA α-methyl proton resonances and $A_{O\text{-}CH3}$ is the area of the O–CH_3 proton resonances in ^{1}H NMR spectra. Activity of complex 1 has been found to be slightly lower in copolymerization reactions compared to its activity toward homopolymerization of the same monomers. Also, average molecular weights of the copolymers are found to be lower than the average molecular weights of the homopolymers [44]. Details of the results of copolymerization are given in Table 5. From the result, it is concluded that polymer yields had an inverse relation with monomer [MA/MMA] ratios.

Characterization

The copolymers were also characterized by gel permeation chromatography (GPC), ^{1}H NMR spectroscopy, and DSC. Gel permeation chromatography was used to determine the

Table 5 Copolymerization of MA and MMA catalyzed by 1 in the presence of $NaBPh_4$ at room temperature (25 °C) in aqueous emulsion in air[a]

Entry	Feed ratio MMA/MA mol/mol	MMA incorporation (%)[a]	M_n[b] ($\times 10^5$)	M_w/M_n[c]	Yield g (%)	Tacticity[c]	Activity[d] ($\times 10^4$)
1	1:4	13.85	9.6	2.1	1.12(63.3)	25:38:37	1.12
2	1:1	71.94	11.3	1.6	1.28(68.8)	45:36:19	1.28
3	4:1	84.05	15.6	1.6	1.53(78.6)	57:33:10	1.53
4	9:1	93.20	16.8	1.7	1.61(81.6)	66:32:2	1.61

Reaction conditions: [1] = [$NaBPh_4$] = 0.002 mol/L, reaction time = 60 min, total monomer concentration (MMA + MA) = 0.4 mol/L

[a] From ^{1}H NMR

[b] GPC

[c] Cosyndiotactic/co-heterotactic/co-isotactic

[d] Gram of polymer per mole of catalyst per hour

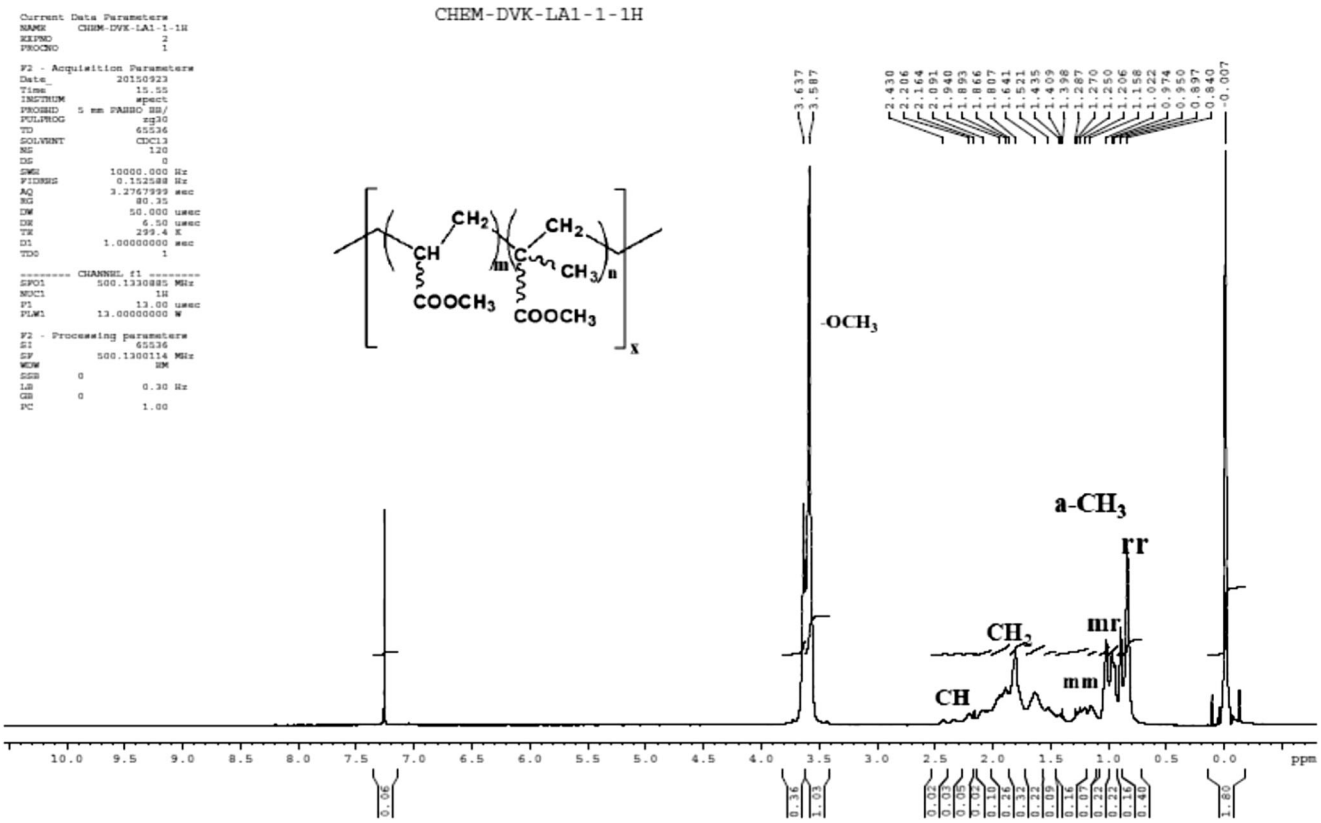

Fig. 12 Representative ^{1}H NMR spectrum of PMA and PMMA synthesized

average molecular weights of the copolymers. The copolymer products exhibit average molecular weights in the range 9.6×10^5 to 16.8×10^5 at different feed ratios. Also, low molecular weight distribution, M_w / Mn ≈ 1.6–2.1 suggests a single species as an active catalytic system for single-site insertive polymerization reactions.

Figure 12 shows the ^{1}H NMR spectrum of the copolymer. The ^{1}H NMR spectral pattern of the copolymer is different from that of homopolymers of MA and MMA. Three peaks which appear at 0.84–1.21 ppm for homo-PMMA due to α-CH_3 protons split into six peaks. These six peaks appearing in the region from δ ~ 1.28–0.85 have been assigned according

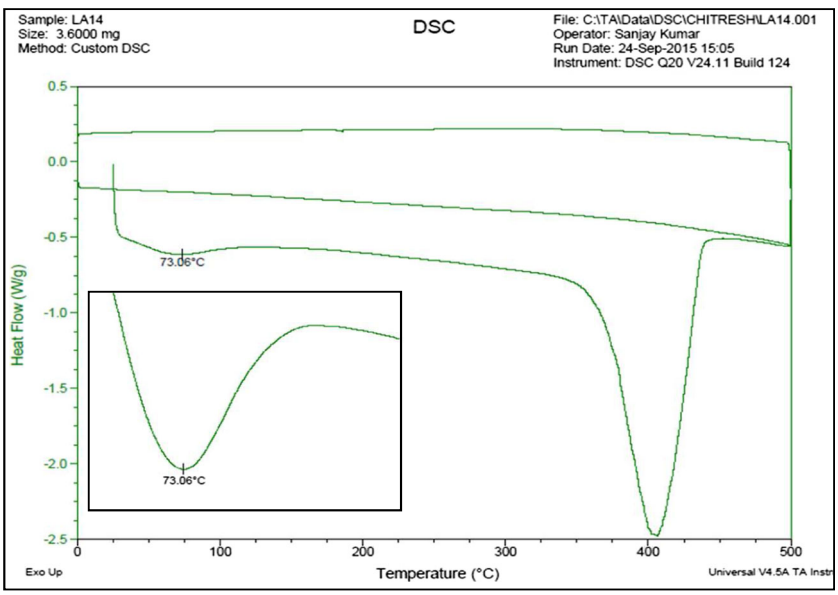

Fig. 13 Representative DSC curve of random MA and MMA copolymers

Table 6 Reactivity ratio values of MA and MMA obtained by different methods

Entry	Method	r_{MA}	r_{MMA}
1	Fineman–Ross	1.96	1.47
2	Kelen–Tudos	1.84	1.39

to literature data, to co-iso [mm], co-hetero [mr], and co-syndio [rr] triads [45]. The intensities of the peaks for α-CH_3 protons decrease as the molar fraction of MMA in the copolymer decreases.

DSC analysis (Fig. 13) reveals only one intermediate glass transition temperature (T_g) for copolymers at 73.06 °C when both the monomers were premixed and added simultaneously in polymerization indicating the formation of a random copolymer. All these analysis techniques (^{1}H NMR, GPC, and DSC) give evidence in support of the formation of copolymers and also suggest that the polymer obtained is not simply a mixture of homopolymers but monomers are chemically bonded to each other after copolymerization reactions.

Determination of monomer reactivity ratios

For predicting the copolymer composition and for understanding the kinetics and mechanistic aspects of copolymerization, monomer reactivity ratios were studied [46]. Three copolymerization reactions were carried out to calculate the reactivity ratios. These reactions were quenched at early stages because if copolymerization is carried to high conversion, significant computational problems may arise to determine the copolymerization parameters. Simple and widely used linear least-square methods (Fineman–Ross and Kelen–Tudos) were used to determine the reactivity ratios of methyl acrylate and methyl methacrylate (details are given in Fig. S9 Supporting Information). The reactivity ratio values obtained (Table 6) by the two methods are in good agreement with each other. From linear plots obtained by two least-square methods, the reactivity ratio values of methyl acrylate and of methyl methacrylate are found to be greater than 1 (r_1, r_2 >1) which suggests that homo-propagation is faster than cross-propagation. Also, reactivity ratio values suggest the tendency of formation of the block copolymer product. Reactivity ratio values (r_1, r_2 >1) obtained from two methods made us curious and interested to synthesize block copolymers.

Block copolymers can be synthesized by sequential addition of monomers. Therefore, MMA was polymerized for the first 30 min, and after that, a second monomer, methyl acrylate, was added. Polymerization reaction was then continued for the next 30 min. The resulting copolymers were washed and purified. The microstructure of the resulting block copolymer was confirmed by differential scanning calorimetry. The analysis reveals two distinct T_g, one at 22.40 °C and another at 137.13 °C (Fig. 14) for high molecular weight syndiotactic-rich PMA and PMMA block copolymers.

Activation energy for the viscous flow of polymer

Viscosity is one of the unique rheological properties of the liquids. Polymer samples can be analyzed by carrying out simple viscometry experiments. Viscosity average molecular

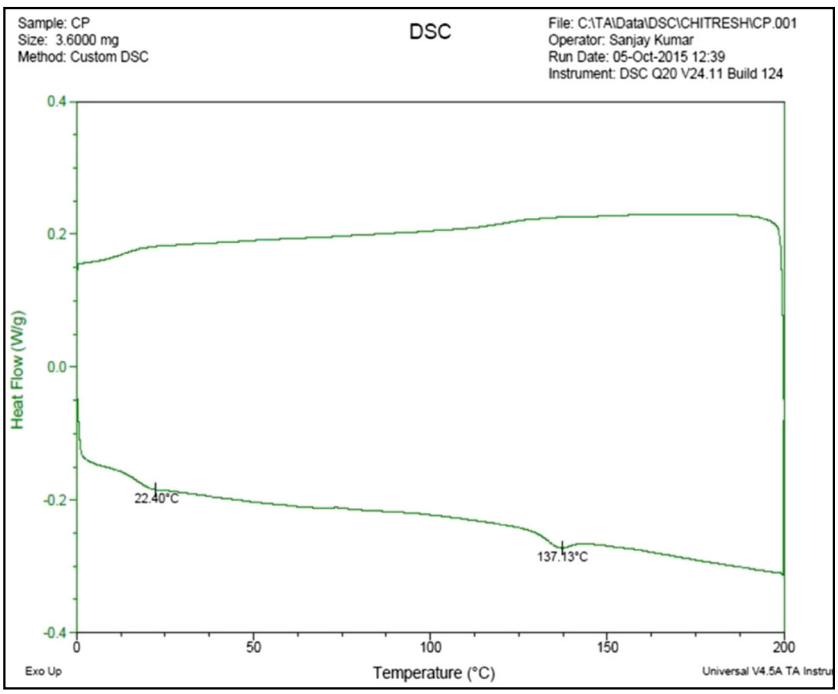

Fig. 14 Representative DSC curve of block copolymer

Table 7 Results of viscosity measurements for PMMA

Concentration, gm/dl	η , mPa s^{-1}		$E_\eta = R\frac{d\ln(\eta)}{d(T^{-1})} = R\frac{\Delta\ln(\eta)}{\Delta(T^{-1})}, \frac{Kcal}{mol}$
	20 °C or 293.15 K	30 °C or 303.15 K	
1	1.89	1.01	11.06
0.6	1.20	0.74	8.51
0.5	0.91	0.60	7.14
0	0.47	0.33	6.27

weight (M_v) can be determined by a glass capillary viscometer using the Staudinger equation and the famous Mark–Houwink equation [44]. Likewise, activation energy of viscous flow (E_a) of the different polymeric solutions of PMMA and PMA was calculated. There are a number of objectives to measure E_a, for diffusion of molecular probes (dyes), to resolve polymeric waste problem by knowing E_a of virgin and discarded polymer samples [47], to find polymer durability [48], to find average molecular weight, and many more. Viscosity is influenced by a number of factors such as concentration and temperature. We have studied the effect of different concentrations of the polymeric samples prepared in acetone on E_a (activation energy) (Fig. S10 (a) and (b), Supporting information).

It has been believed that the activation energy for the viscous flow of polymer solutions had a direct relation with polymer concentrations. The apparent activation energy for the viscous flow of a polymer solution, *Ea* or *Eη*, is defined by the following equation [49].

$$Ea = E_\eta = R\frac{d\ln(\eta)}{d(T^{-1})} = R\frac{\Delta\ln(\eta)}{\Delta(T^{-1})}, \frac{Kcal}{mol} \quad (2)$$

where

η is the viscosity coefficient of the solution at temperature T and R is the gas constant $R = 1.987 \times 10^{-3}\frac{Kcal}{K.mol}$.

The viscosity coefficient of a given polymer is a function of the polymer concentration c (in g/dl) and the absolute temperature T.

The average molecular weight of polymers is one of the important variables affecting the viscous flow of polymer melt. The most reliable relation between high molecular weight polymers in the range of 10^3 and above with limiting viscosity (η) [50] is given as

$$\eta \propto M_w \quad (3)$$

From the apparent activation energy equation 2, it is found that limiting viscosity has a direct relation with E_a. It was summarized in Tables 7 and 8 that apparent activation energy increases with increase in limiting viscosity of the polymer solution at varying concentrations. Therefore, it is concluded that as the limiting viscosity and activation energy increase, average molecular weight also increases. Activation energy calculated for polymethyl acrylate is higher than that for polymethyl methacrylate which is also evidence in support of high molecular weight polymer in addition to viscosity average molecular weight (M_v).

Characteristics of the polymer latex particle

The characteristic of polymer latex has also been studied using DLS, high-resolution transmission electron microscopy (HRTEM), and field emission scanning electron microscopy (FESEM). Another interesting feature of the present catalytic system is that it produces a stable latex containing polymer particles in nano dimensions. The

Table 8 Results of viscosity measurements for PMA

Concentration, gm/dl	η , mPa s^{-1}		$E_\eta = R\frac{d\ln(\eta)}{d(T^{-1})} = R\frac{\Delta\ln(\eta)}{\Delta(T^{-1})}, \frac{Kcal}{mol}$
	20 °C or 293.15 K	30 °C or 303.15 K	
1	7.60	2.80	17.58
0.6	2.69	1.69	8.23
0.5	1.70	1.18	6.44
0	0.46	0.33	5.82

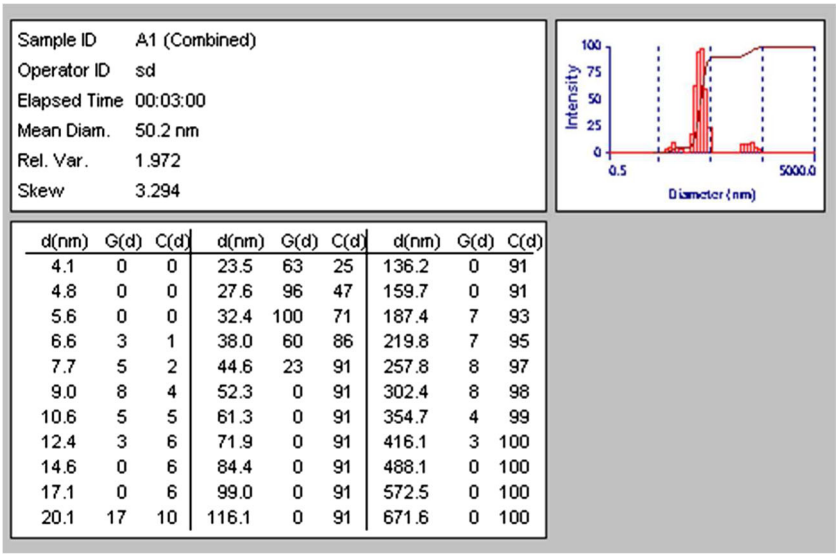

d(nm)	G(d)	C(d)	d(nm)	G(d)	C(d)	d(nm)	G(d)	C(d)
4.1	0	0	23.5	63	25	136.2	0	91
4.8	0	0	27.6	96	47	159.7	0	91
5.6	0	0	32.4	100	71	187.4	7	93
6.6	3	1	38.0	60	86	219.8	7	95
7.7	5	2	44.6	23	91	257.8	8	97
9.0	8	4	52.3	0	91	302.4	8	98
10.6	5	5	61.3	0	91	354.7	4	99
12.4	3	6	71.9	0	91	416.1	3	100
14.6	0	6	84.4	0	91	488.1	0	100
17.1	0	6	99.0	0	91	572.5	0	100
20.1	17	10	116.1	0	91	671.6	0	100

Fig. 15 Representative hydrodynamic size distribution of latex particles of PMMA measured by DLS

aliquots were taken from the polymerization mixture and characterized by DLS, HRTEM, and FESEM. The DLS studies show that the mean diameter of the latex particles lies around 50 nm (Fig. 15). Further, the stability of the polymer latex containing polymer nanoparticles was also determined by keeping the latex undisturbed for nearly 6 months; hardly any change in the hydrodynamic diameter of the polymer particles was observed. Thus, it is concluded that the present system affords stable polymer latex containing nano range polymer particles.

A finding of the DLS study was further supported by HRTEM and FESEM analysis (Fig. 16a, b). From HRTEM of a very dilute latex sample, a chain-like structure of polymer particles having a diameter less than 100 nm is visualized. It is also evident from FESEM that the polymer particles are of spherical nature having a diameter less than 50 nm.

Proposed mechanism

Based on a careful survey of literature on aqueous solution chemistry of the early transition metals and experimental findings of the mechanistic investigations reported in our previous study [22, 23], it is expected that the newly synthesized [ONNO]-type titanium(IV) complex, $TiLCl_2$ {*LH_2=2-(3,5-Di-tert-butyl-2-hydroxy-benzylamino)-succinamic acid*} upon addition to water undergoes rapid chloride hydrolysis to produce $[LTi(OH)(OH_2)]^+$ as the major species. Tetraphenylborate is added to stabilize this cationic species by forming a tight ion pair in the solvent cage and to help the cationic species to enter inside the micelles through the negatively charged outer surface of SDS (Scheme 3). Now, in the presence of olefins, chain growth occurs through exchange of water for olefinic monomer followed by a monometallic GTP-like insertion sequence [44] (Scheme 4) to produce

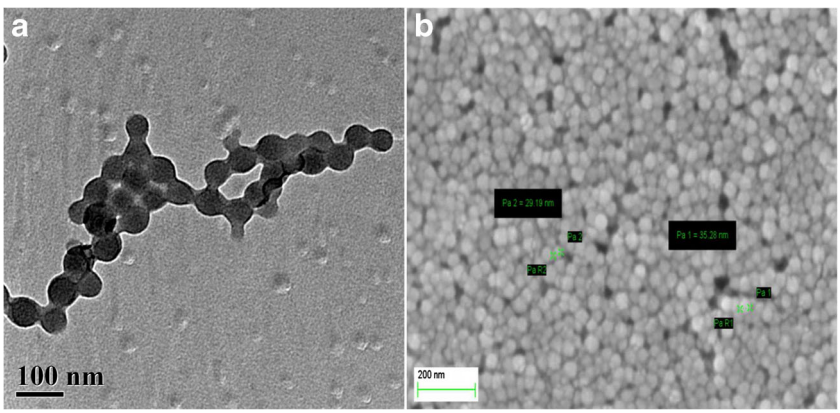

Fig. 16 **a** HRTEM image of PMMA NPs synthesized. **b** FESEM image of PMMA NPs synthesized

Scheme 3

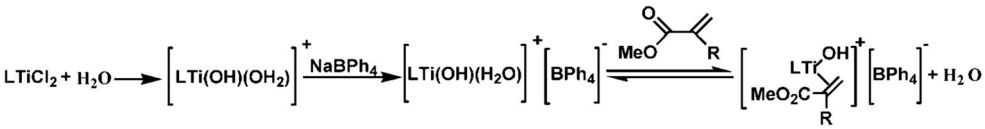

PMMA/PMA with a –OH group at the chain end. This proposal is experimentally supported by the fact that the trichloroacetyl isocyanate derivatives of the polymer samples show a peak around 9.15 ppm in the ^{1}H NMR spectrum for the imidic proton confirming the presence of the –OH end group (Scheme S1 and Fig. S11, Supporting information).

Comparison between [TiLCl$_2$(THF)]{LH$_2$=*S*(-) 2-(3,5-Di-tert-butyl-2-hydroxy-benzylamino) -3-methyl-butyric acid} and TiLCl$_2$ {LH$_2$=2-(3, 5-Di-tert-butyl-2-hydroxy-benzylamino)-succinamic acid} catalytic systems

The efficiency of the present L-asparagine-based titanium catalyst has been compared with the previously reported [21] L-valine-based titanium complex (Table 9). It has been found that the newly synthesized [ONNO]-type titanium(IV) complex, TiLCl$_2$ {*LH$_2$=2-(3,5-Di-tert-butyl-2-hydroxy-benzylamino)-succinamic acid*}, having an extra donor arm shows higher activity in the order of 10^4 in comparison to the [ONO]-type titanium(IV) complex [TiLCl$_2$(THF)] {*LH$_2$=S(-)2-(3,5-Di-tert-butyl-2-hydroxy-benzylamino)-3-methyl-butyric acid*} having activity in the order of 10^3. This may be explained by the fact that the side arm N remains attached to the metal center and thus lowers the electrophilicity of the titanium center. Hence, the rate of hydrolysis becomes slower and the [ONNO]-type complex becomes more stable than the [ONO]-type complex. It may be noted that in the presence of air, the yield and average molecular weight of the polymeric product obtained by the [ONNO]-type titanium(IV) catalyst is found to be much higher than the [ONO]-type tridentate titanium(IV) complex. Even in the presence of argon atmosphere, the [ONO]-type titanium(IV) complex is not reported to produce much higher yield. Moreover, the stereoselectivity of the present catalytic system in polymerization reactions is almost comparable to [LTiCl$_2$(THF)] complex, producing 64 % syndiotactic PMMA and 66 % co-syndiospecific MMA units in copolymers.

Conclusion

In summary, we have synthesized a new phenoxy amine-based [ONNO]-type ligand system with a sidearm approach from readily available starting materials. Titanium complex bearing this ligand system was obtained in a single-step procedure in the presence of THF as a solvent. The catalytic potential of the complex was studied by catalyzing aqueous emulsion polymerization of polar olefins (methyl acrylate and methyl methacrylate) at room temperature. In the presence of NaBPh$_4$, the complex affords high molecular weight polymers with narrow polydipersity index. Activation energy for the viscous flow of the polymers is also found to be higher which also supports the higher molecular weight of the polymers. The yield of the polymeric products has been found to be higher even in the presence of oxygen when no inert environment is provided. Due to the influence of the pendant donor group, the activity of the present catalytic system has been found to be much higher than the previously reported catalytic systems. In addition to homopolymerization, the complex also shows good capability for copolymerization of methyl acrylate with methyl methacrylate. Also, block copolymers could be synthesized by sequential addition of monomers. Therefore, it is a simple and environment-friendly way to carry out aqueous polymerization reactions in contrast to Ziegler Natta catalysis which involves organic solvents and hazardous MAO.

Scheme 4 The proposed monometallic GTP-like methyl methacrylate polymerization pathways traversed by single-site early-transition metal catalysts

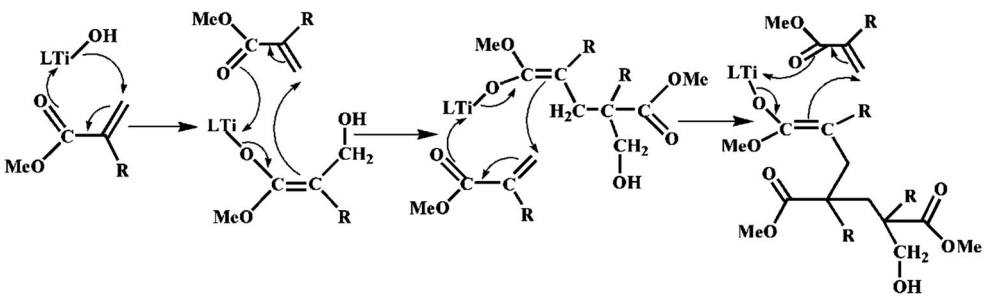

Table 9 Comparison between $[LTiCl_2]$[a] and $[LTiCl_2(THF)]$ catalyzed homopolymerization of MMA in the presence of $NaBPh_4$ at room temperature (25 °C) in aqueous emulsion[c]

Entry	Catalyst	Atmosphere	Polymer	Time	Yield (%)	M_n (10^5)[a]	M_w/M_n	Activity[b]
1	$[LTiCl_2]$	Air	PMMA	5	49.0	5.10	1.6	11.76×10^4
2	$[LTiCl_2(THF)]$	Air	PMMA	5	6.0	1.95	1.6	14.4×10^3
3	$[LTiCl_2(THF)]$	Argon	PMMA	5	15.6	5.62	1.6	37.4×10^3

Reaction conditions: $[LTiCl_2] = [NaBPh_4] = 0.002$ mol/L, monomer concentration (with respect to catalyst) 0.5 mol%

[LTiCl2]{L=2-(3, 5-Di-tert-butyl-2-hydroxy-benzylamino)-succinamic acid}, *[$LTiCl_2$ (THF)]*{L=2-(3,5-Di-tert-butyl-2-hydroxy-benzylamino)-3-methyl-butyric acid}

[a] GPC

[b] Gram of polymer per mole of catalyst per hour

Acknowledgments We thank Dr. M. Baidya, Department of Chemistry, IIT Madras, and Mr. Chitresh Kumar Bhargava, Research Fellow, Department of Chemical Engineering, IIT Bombay, for providing some of the characterizations presented in this paper.

Compliance with ethical standards No human and animals were involved in the present study.

Funds This study was funded by Jaypee University of Engineering and Technology, Guna, 473226, India.

Conflict of interest The authors declare that they have no conflict of interest.

References

1. Brintzinger HH, Fischer D, Mulhaupt R, Rieger B, Waymouth RM (1995) Stereospecific olefin polymerization with chiral metallocene catalysts. Angew Chem 34:1143–1170
2. Landfester K, Tiarks F, Hentze HP, Antonietti M (2000) Polyaddition in miniemulsions: a new route to polymer dispersions. Macromol Chem Phys 1–5
3. Bauers FM, Mecking S (2001) Aqueous homo and copolymerization of ethylene by neutral nickel (II) complexes. Macromolecules 34:1165–1171
4. Mulhaupt R (2003) Catalytic polymerization and post polymerization catalysis fifty years after the discovery of Ziegler's catalysts. Macromol Chem Phys 204:289–327
5. Ittel SD, Johnson LK, Brookhart M (2000) Late-metal catalysts for ethylene homo and copolymerization. Chem Rev 100:1169–1204
6. Mecking S (2001) Olefin polymerization by late transition metal complexes—a root of Ziegler catalysts gains new ground. Angew Chem In Ed 40:534–540
7. Tomov A, Broyer JP, Spitz R (2000) Emulsion polymerization of ethylene in water medium catalysed by organotransition metal complexes. Macromol Symp 150:53–58
8. Lindner E, Schmid M, Wald J, Queisser JA, Geprägs M, Wegner P, Nachtigal C (2000) Catalytic activity of cationic diphospalladium(II) complexes in the alkene/CO copolymerization in organic solvents and water in dependence on the length of the alkyl chain at the phosphine ligands. J Organomet Chem 602:173–187
9. Hustad PD, Coates GW (2002) Insertion/isomerization polymerization of 1,5-hexadiene: synthesis of functional propylene copolymers and block copolymers. J Am Chem Soc 124:11578–11579
10. Jones DJ, Gibson VC, Green S, Maddox PJ (2002) Discovery of a new family of chromium ethylene polymerization catalysts using high throughput screening methodology. Chem Commun 1038–1039.
11. Younkin TR, Connor EF, Henderson JI, Friedrich SK, Grubbs RH, Bansleben DA (2000) Science neutral, single-component nickel (II) polyolefin catalysts that tolerate heteroatoms. Science 287(5452): 460–462
12. Wang C, Sun X-L, Guo Y-H, Gao Y, Li B, Ma Z, Xia W, Shi L-P, Tang Y (2005) Novel titanium catalysts bearing an [O,N,S] tridentate ligand for ethylene homo and copolymerization. Macromol Rap Commun 26:1609–1614
13. Zhang X, Liu Z, Yi J, et al. (2013) The investigation of novel non-metallocene catalysts with phenoxy-imine ligands for ethylene (co-) polymerization. Polym Int 62:419–426
14. Meppelder GJM, Fan HT, Spaniol TP, Okuda J (2009) Synthesis, structure and olefin polymerization activity of titanium complexes bearing asymmetric tetradentate [OSNO] -type bis (phenolato) ligands. Inorg Chem 48:7378–7388
15. Ciancaleoni G, Fraldi N, Budzelaar Peter HM, Busico V, Macchioni A (2011) Structure and dynamics in solution of bis (phenoxy-amine) zirconium catalysts for olefin polymerization. Organometallics 30:3096–3105
16. Wang C, Ma Z, Sun X-L, Gao Y, Guo Y-H, Tang Y, Shi L-P (2006) Synthesis and characterization of titanium (IV) complexes bearing monoanionic [ONX] (X= O, S, Se) tridentate ligands and their behaviors in ethylene homo- and co-polymerization with 1-hexene. Organometallics 25:3259–3266
17. Chan Michael CW, Tam KH, Zhu N, Chiu P, Matsui S (2006) Synthesis, structures and olefin polymerization characteristics of group 4 catalysts [Zr{(OAr)2py}Cl2 (D)](D) O-donors, Cl[HPR3] supported by tridentate pyridine-2,6-bis (aryloxide) ligands. Organometallics 25:785–792
18. Makio H, Fujita T (2004) Observation and identification of the catalytically active species of bis(phenoxy-imine) group 4 transition metal complexes for olefin polymerization using 1H NMR spectroscopy. Macromol Symp 213:221–234
19. Foley SR, Stockland RA, Jr Shen H, Jordan RF (2003) Reaction of vinyl chloride with late transition metal olefin polymerization catalysts. J Am Chem Soc 125:4350–4361

20. Foley SR, Stockland RA, Jordan RF (2003) Reaction of vinyl chloride with group 4 metal olefin polymerization catalysts. J Am Chem Soc 125:796–809
21. Roman JS, Valero M (1990) Quantitative evolution of sequence distribution and stereoregularity in ethyl acrylate-methyl methacrylate copolymer by 13Cn.m.r spectroscopy. Polymer 31
22. De SK, Bhattacharjee M (2013) Titanium (IV) nonmetallocene complex catalyzed aqueous homopolymerization and copolymerization of styrene and methyl methacrylate: an environmentally friendly approach to ultrahigh molecular weight polymer nanoparticles. J Poly Sci Part A: Poly Chemistry 51:1540–1549
23. Sharma K, Lunawat G, De SK (2016) Environmentally benign stereoselective polymerizations of polar as well as nonpolar olefins by a new postmetallocene Ti(IV) salicylate complex at ambient temperature in aqueous emulsion. J Polym Res 23:41
24. Clark RJH (1965) Metal-halogen stretching frequencies in inorganic complexes. Spectrochim Acta 21:955–963
25. Seetharamappa J (1999) Synthesis, structural and thermal studies of titanium (IV) complexes of N-alkyl phenothiazines. Turk J Chem 23:429–434
26. Buettner KM, Valentine AM (2012) Bioinorganic chemistry of titanium. Chem Rev 112:1863–1881
27. Toney JH, Marks TJ (1985) Hydrolysis chemistry of the metallocene dichlorides equilibria and mechanistic implications for a new class. J Am Chem Soc 107:947–953
28. Bhattacharjee M, Patra BN (2004) [Cp2TiCl2] as polymerization catalyst in aqueous medium: polymerization of styrene in water. J Organomet Chem 689:1091–1094
29. Bhattacharjee M, Patra BN (2004) [Cp2TiCl2] catalyzed polymerization in water: polymerization of methyl methacrylate to a high molecular weight polymer. Polymer 45:3111–3114
30. Patra BN, Bhattacharjee M (2005) Early transition metal catalyzed aqueous emulsion copolymerization: copolymerization of styrene and methyl methacrylate by Cp2TiCl2 in aqueous medium. J Polym Sci Polym Chem 43:3707–3710
31. Tian J, Coates GW (2000) Development of a diversity-based approach for the discovery of stereoselective polymerization catalysts: identification of a catalyst for the synthesis of syndiotactic polypropylene. Angew Chem Int Ed 39:3626–3629
32. Tshuva EY, Goldberg I, Kol M (2000) Isospecific living polymerization of 1-hexene by a readily available nonmetallocene C2-symmetrical zirconium catalyst. J Am Chem Soc 122:10706–10707
33. Wagner HL (1985) The Mark-Houwink-Sakurda equation for the viscosity of linear polyethylene. J Phys Chem Data 14:2
34. Kawamura T, Toshima N, Matsuzaki K (1993) Assignment of finely resolved 13C NMR spectra of poly(methyl methacrylate). Makromol Chem Rap Commun 14:719–724
35. Sankar V, Kumar TS, Rao KP (2004) Preparation, characterisation and fabrication of intraocular lens from photo initiated polymerised poly (methyl methacrylate). Trends Biomater. Artif Organs 17:24–30
36. Matsuzaki K, Kanai T, Kawamura T, Matsumoto S, Uryu T (1973) 13C nuclear magnetic resonance spectra of polyacrylates and their model compounds. J Polym Sci Part A: Chem Ed 11:961–969
37. Li Q, Bao Y, Wang H, Du F, Li Q, Jin B, Bai R (2013) A facile and highly efficient strategy for esterification of poly (meth) acrylic acid with halogenated compounds at room temperature promoted by 1, 1, 3, 3-tetramethylguanidine. Polym Chem 4:2891–2897
38. Karasz FE, MacKnight WJ (1968) The influence of stereoregularity on the glass transition temperature of vinyl polymers. Macromolecules 1:537–540
39. Wood LA (1958) Glass transition temperatures of copolymers. J Polym Sci 28:319–330
40. Shirai M, Kawaue A, Okamura H, Tsunooka M (2004) Synthesis of novel photo-cross linkable polymers with redissolution property. Polym 45:7519–7527
41. Barim G, Yayla MG, Degirmenci M (2014) Copolymerization of 4-acetylphenyl methacrylate with ethyl methacrylate: synthesis, characterization, monomer reactivity ratios and thermal properties. Int J Polym Sci 17:610–616
42. Shipp DA, Wang JL, Matyjaszewski K (1998) Synthesis of acrylate and methacrylate block copolymers using atom transfer radical polymerization. Macromolecules 31:8005–8008
43. Terao H, Ishii S, Mitani M, Tanaka H, Fujita T (2008) Ethylene/polar monomer copolymerization behavior of bis(phenoxy–imine) Ti complexes: formation of polar monomer copolymers. J Am Chem Soc 130(52):17636–17637
44. Jensen TR, Yoon SC, Dash AK, Luo L, Marks TJ (2003) Organotitanium-mediated stereoselective coordinative/insertive homopolymerizations and copolymerizations of styrene and methyl methacrylate. J Am Chem Soc 125:14482–14494
45. Lopez-Gonzalez MMC, Fernandez-Garcia M, Barrales-Rienda JM, Madruga EL (1993) Sequence distribution and stereoregularity in methyl methacrylate-methyl acrylate copolymers at high conversions. Polymer 34:3123–3128
46. Lianga SJ, Dengb J-p, Yang W-t (2010) Monomer reactivity ratio and thermal performance of α-methyl styrene and glycidyl methacrylate copolymers. Chinese J Polym Sci 28:323–330
47. Al-Furhood JA, Alsewailem FD, Almutabaqani LA (2014) Activation energy for the pyrolysis of polymer wastes. Eur Chem Bull 3:93–97
48. Ding S, khare A, Ling Michael TK, Sandford C, Woo L (2001) Polymer durability estimates based on apparent activation energies for thermal oxidative degradation. Thermochim Acta 367-368:107–112
49. Okada R, Tanzawa H (1965) Apparent activation energy for the viscous flow of polymer solutions. J Polym Sci A3: Issue no. 12
50. Lu QW, Hernandez-Hernandez ME, Macosko CW (2003) Explaining the abnormally high flow activation energy of thermoplastic polyurethanes. Polymer 44:3309–3318